UNIVERSIDADE DE LISBOA

INSTITUTO SUPERIOR TÉCNICO

Università degli Studi di Padova

Tokamak Magnetic Control Simulation: Applications for JT60-SA and ISTTOK Operation.

Doménica Corona Rivera

Supervisor:Prof. Horácio Fernandes

Co-Supervisor: Prof. Nuno Cruz

External supervisor: Prof. Alfredo Pironti

Thesis specifically prepared to obtain the PhD Degree in

Technological Physics Engineering

Month 2020

ABSTRACT

Abstract en ingles

Keywords:Real-time control, plasma current, centroid position, state-space

RESUMO

Abstract em tuga

Palavras-chave:

SOMMARIO

Abstract em italiano

Parole chiave:

ACKNOWLEDGEMENTS

This work was supported by Fundação para a Ciência e a Tecnologia (FCT) under the grant No.**PD/BD/114306/2016** carried out as part of the training in the framework of the Advanced Program in Plasma Science and Engineering (APPLAuSE, sponsored by FCT under grant No. PD/00505/2012).

CONTENTS

1 INTRODUCTION 3

1.1 Tokamak plasma control 3

1.2 Behind the plasma current 3

1.3 Thesis outline 3

2 PLASMA CONTROL SYSTEMS 5

2.1 Overview of control systems 5

2.1.1 DIII-D Plasma Control System 5

2.1.2 Systéme de Contrôle Distribué 7

2.2 MARTe framework 7

2.2.1 MARTe architecture 8

2.2.2 Hardware containers 8

2.2.3 MARTe 2.0 9

2.3 Equilibrium and control algorithms 9

2.3.1 State-Space models 9

2.3.2 PID control 9

2.3.3 Multiple-Input Multiple-Output control 9

3 JT60-SA CONTROL DESIGN 11

3.1 Machine description 11

3.2 CREATE tools 11

3.3 Controller design 11

3.3.1 eXtreme Shape Controller 11

3.4 QST tools implementation 11

3.4.1 CCS 11

3.4.2 QST magnetic controller (FBC) 11

3.5 Simulation results 12

3.5.1 ELM 12

3.5.2 Compound ELM 12

3.5.3 Minor Disruption 12

4 ISTTOK 15

4.1 Machine description 15

4.2 Diagnostics and Actuators 15

4.3 ATCA-MIMO-ISOL boards 15

4.3.1 Hardware layout 15
4.3.2 Real-time integration software 15
4.4 Plasma current magnetic field 15
4.5 Plasma centroid position determination 15
5 ISTTOK RESULTS 17
5.1 Implementation of the General Application Modules 17
5.1.1 PID control implementation 17
5.1.2 Data-driven state-space model retrieving 17
5.1.3 Kalman filter implementation 17
5.1.4 Multiple-Input Multiple-Output control implementation 17
5.2 Plasma curruent centroid position control results 17
5.2.1 PID control and LQR control results 17
6 CONCLUSIONS 27
Bibliography 30
A EXTENDED CONTROL RESULTS 31
B FBC CONTROLLER AND CCS CONFIGURATION 45

LIST OF FIGURES

Figure 2.1 DIII-D digital PCS in 1991 [2]. 6

Figure 2.2 Actual DIII-D PCS real-time systems [4]. 6

Figure 2.3 TCV SCD. Real-time network nodes connection. The nodes configurations are shown together with the typical diagnostic and actuator systems to which they are connected [7]. 7

Figure 2.4 Example of a set of GAMs connected to the DDB. Timing and hardware GAMs provide the I/O interface to the exterior, whereas a generic waveform GAM inputs the reference for a PID controller. Finally, the output is sent to a DAC and the data is stored for analysis by a collection GAM. It should be noticed that the reference generation and the controller GAM are not aware of the changes in the data providers and data consumers. [11] 8

Figure 3.1 JT60-SA tokamak configuration 12

Figure 3.2 JT-60SA poloidal cross-section and layout of the Poloidal Field coils system [14]. 13

Figure 5.1 ISTTOK MARTe overall scheme 18

Figure 5.2 Fig. 18

Figure 5.3 Fig. 19

Figure 5.4 Pole-Zero maps in closed loop for the model when $I_p \approx 4kA$. Superposition of poles and zeros can be seen in the four transfer functions. 19

Figure A.1 Plasma centroid position Shot# 48563 Shot# 48561 32

Figure A.2 lalala Shot# 48563 Shot# 48561 32

Figure A.3 Plasma centroid position Shot# 48556 Shot# 48552 33

Figure A.4 lalala Shot# 48556 Shot# 48552 33

Figure A.5 Plasma centroid position Shot# 48551 Shot# 48554 34

Figure A.6 lalala Shot# 48551 Shot# 48554 34

Figure A.7 Plasma centroid position Shot# 48515 Shot# 48541 35

Figure A.8 lalala Shot# 48515 Shot# 48541 35

Figure A.9 Plasma centroid position Shot# 48544 Shot# 48542 36

Figure A.10 lalala Shot# 48544 Shot# 48542 36

Figure A.11 Plasma centroid position Shot# 48546 Shot# 48548 37

Figure A.12 lalala Shot# 48546 Shot# 48548 37

Figure A.13 Plasma centroid position Shot# 48340 Shot# 48338 38

Figure A.14 lalala Shot# 48340 Shot# 48338 38

Figure A.15 Plasma centroid position Shot# 48343 Shot# 48342 39
Figure A.16 lalala Shot# 48343 Shot# 48342 39
Figure A.17 Plasma centroid position Shot# 48346 Shot# 48345 40
Figure A.18 lalala Shot# 48346 Shot# 48345 40
Figure A.19 Plasma centroid position Shot# 48349 Shot# 48348 41
Figure A.20 lalala Shot# 48349 Shot# 48348 41
Figure A.21 Plasma centroid position Shot# 48352 Shot# 48354 42
Figure A.22 lalala Shot# 48352 Shot# 48354 42
Figure A.23 Plasma centroid position Shot# 48351 Shot# 48350 43
Figure A.24 lalala Shot# 48351 Shot# 48350 43

LIST OF TABLES

Table 5.1 Centroid position RMSE comparison between PID and MIMO-LQR controlled discharges for different set points and plasma current scenarios. 26

LIST OF ABBREVIATIONS

@TODO: Review variable lists as writing the thesis

- AC - Alternating Current
- ADC - Analog to Digital Converter
- ATCA - Advanced Telecommunications Computing Architecture
- CREATE - Consorzio di Ricerca per l'Energia, l'Automazione e le Tecnologie dell'Elettromagnetismo
- DAC - Digital to Analog Converter
- EO - Electronic Offset
- GAM - Generic Application Module
- IST - Instituto Superior Técnico
- LQR - Linear Quadratic Regulator
- MARTe - Multi-threaded Application Real-Time executor
- MIMO - Multiple-Input Multiple-Output
- PCS - Plasma Control System
- PF - Poloidal Field
- PID - Proportional - Integrative - Derivative
- RFM - Reflective Memory
- SCD - Systéme de Contrôle Distribué
- XSC - eXtreme Shape Controller
- WO - Wiring Offset

LIST OF VARIABLES

@TODO: Review variable lists as writing the thesis

VARIABLES:

- I_p - Plasma current
- B_p - Poloidal magnetic field
- μ_0 - Vacuum permeability

1

INTRODUCTION

1.1 TOKAMAK PLASMA CONTROL

1.2 BEHIND THE PLASMA CURRENT

1.3 THESIS OUTLINE

2

PLASMA CONTROL SYSTEMS

2.1 OVERVIEW OF CONTROL SYSTEMS

The control of plasma position, shape and current among other parameters is one of the crucial engineering problems for present and future magnetic confinement devices. The Plasma Control Systems (PCS) lead with the overall control of fusion devices being responsible also for the plasma configuration and scenarios algorithms [1, Chapter 8]. Currently different PCS's are use in the tokamaks around the world. In this chapter the "DIII-D-like" PCS, the Systéme de Contrôle Distribué (SCD) and the Multi-threaded Application Real-Time executor (MARTe) will be approach, this last one being of special interest due to its extensive utilization in this work.

2.1.1 *DIII-D Plasma Control System*

The DIII-D-like PCS is use in various fusion research facilities such as EAST(China), K-STAR (South Korea) and MAST (UK). Early documentation regarding the PCS in DIII-D[1] reefers to digitalization of analog signals transmitted to a high speed processor executing a shape control algorithm and then writing the result to a digital to analog converter for driving the controlled systems . The real-time computer used allowed to performed operations with vectors and matrices required for the plasma shape control algorithm [2]. Figure 2.1 shows the block diagram of the DIII-D PCS 30 years ago.

In recent years the DIII-D PCS had extensive software and hardware upgrades. The PCS actual software consists of an infrastructure library core which provides all the routines that are necessary for implementing a basic and generic control system. The current PCS hardware configuration uses a collection of Intel Linux based multi-processor computers running in parallel to perform the real-time analysis and feedback control [3]. New digitizers have been added to the real-time network to increase the number of signals acquired an to control hardware on real-time, several real-time control algorithms were added and real-time data was added to external entities such as web server. [4]. In

1 DIII-D is a D-shape tokamak operated by General Atomics in San Diego, California.

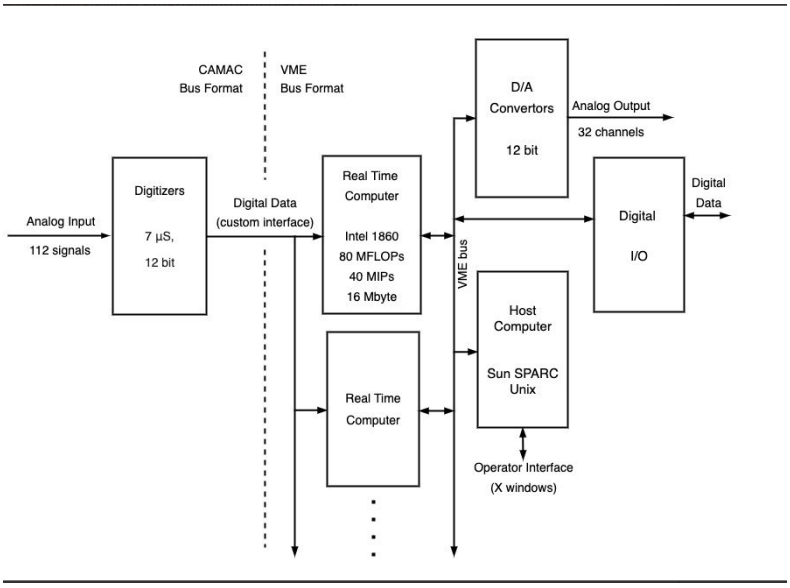

Figure 2.1.: DIII-D digital PCS in 1991 [2].

the current version of the PCS, a Myricom[2] network has been replaced with a 40 Gb/sec InfiniBand[3] network based on the Mellanox Connect-X 3[4] hardware set. Figure 2.2 shows the currently overall networking diagram of DIII-D PCS .

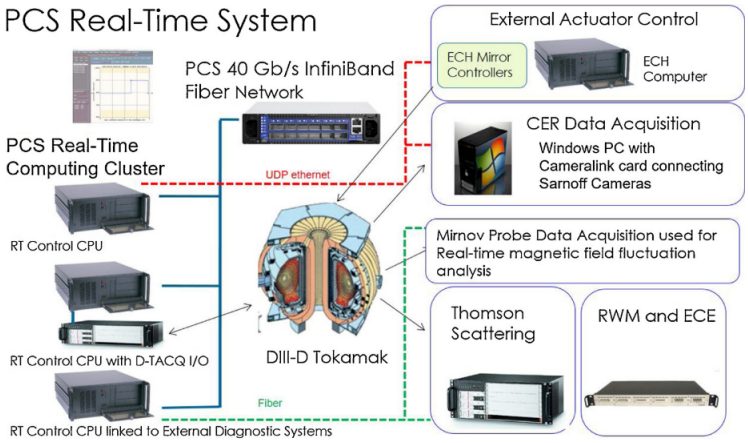

Figure 2.2.: Actual DIII-D PCS real-time systems [4].

2 Myricom networks also called Myrnet are high speed networking systems used to interconnect machines to form computer clusters.
3 Is a network architecture from Mellanox designed to support I/O connectivity and reliability, availability, and serviceability Internet requirements [5].
4 The Connect-X from the Mellanox company are Ethernet network interface cards with PCI Express.

2.1.2 *Systéme de Contrôle Distribué*

The TCV[5] distributed control system uses a modular network of real time PC nodes liken by a real time network to provide feedback control over all of the actuator systems. Each node consists of a Linux PC either embedded on a Compact-PCI module or as a desktop computer with Intel CPU. A fiber optic ring network links the reflective memory (RFM) network cards in each node [6]. The design of the diagnostic signal processing and control algorithms is performed in Matlab-Simulink software. During the real-time execution C/C++ code is generated from the Simulink and compiled into a Linux shared library and distributed to target nodes providing the input/output interface to the control algorithm code [7]. Figure 2.3 depicts the TCV SCD layout with the connectivity to diagnostics and actuators.

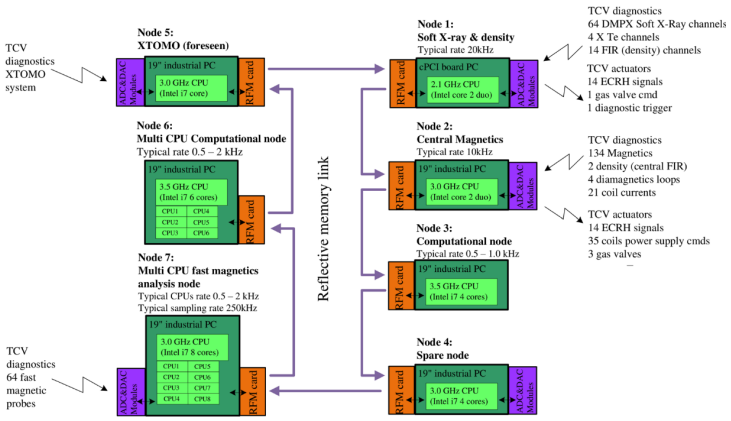

Figure 2.3.: TCV SCD. Real-time network nodes connection. The nodes configurations are shown together with the typical diagnostic and actuator systems to which they are connected [7].

2.2 MARTE FRAMEWORK

Regardless the nature of a real-time system the design of it is usually related to the specific requirements it has, commonly this implies to have customized hardware and software which causes a lack in modularity and portability. When systems become bigger is convenient to provide a common library containing shareable functionalities and which also allows for modular implementations. In order to deal with this the MARTe framework was designed about a decade ago. MARTe was developed in order to standardize general real-time control systems for the execution of control algorithms and is based on a multiplatform C^{++} library [8]. Previous implementations for a software framework similar to MARTe were developed some years before for the JET tokamak. JETRT was a software framework used to develop real-time control and data acquisition systems which laid the foundation for current MARTe framework [9]. MARTe is currently used in several tokamaks such as JET, FTU, COMPASS and ISTTOK.

5 The Tokamak á configuration variable (TCV) is a medium size tokamak localized in Laussane,Switzerland. It is characterized by a highly elongated, rectangular vacuum vessel.

2.2.1 *MARTe architecture*

The unitary MARTe component is the Generic Application Module (GAM), each of the C++ programmed GAMs usually performs an specific task of the control system, the collection of interconnecting GAMs builds MARTe [10]. The GAMs have an entry point to receive data driven configuration and a set of input and output channels to interface with other GAMs. The Dynamic Data Buffer (DDB) is a generic memory data bus where each GAM receives and produce data using DDB named channels. Usually each GAM is associated with a special function of the system like processing data of an specific diagnostic or perform some control algorithm. MARTe hardware data interface and synchronization for inputs and outputs is performed using a special GAM called IOGAM .

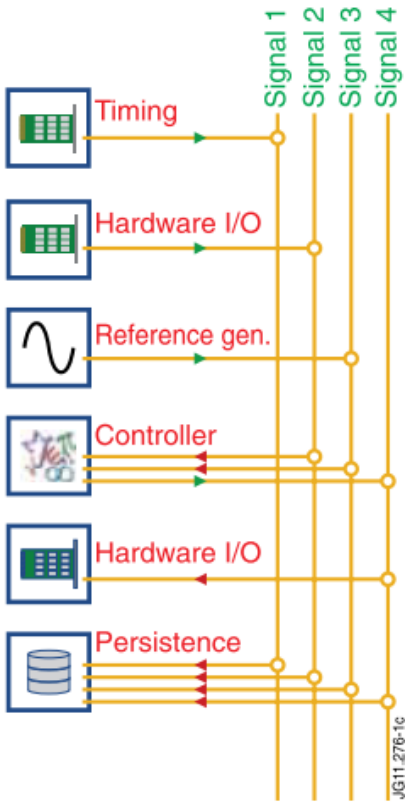

Figure 2.4.: Example of a set of GAMs connected to the DDB. Timing and hardware GAMs provide the I/O interface to the exterior, whereas a generic waveform GAM inputs the reference for a PID controller. Finally, the output is sent to a DAC and the data is stored for analysis by a collection GAM. It should be noticed that the reference generation and the controller GAM are not aware of the changes in the data providers and data consumers. [11]

2.2.2 *Hardware containers*

The MARTe hardware containers

2.2.3 *MARTe 2.0*

Software Quality Assurance (QA) processes are being applied to the development of a new version of the MARTe framework also called MARTe 2.0.
[12]

2.3 EQUILIBRIUM AND CONTROL ALGORITHMS

The RAPTOR (RApid Plasma Transport simulatOR) code is a model-based control-oriented code that predicts tokamak plasma profile evolution on real-time. [13]

2.3.1 *State-Space models*

2.3.2 *PID control*

Proportional-Integral-Derivative (PID) control

2.3.3 *Multiple-Input Multiple-Output control*

Multiple-Input Multiple-Output (MIMO)

3

JT60-SA CONTROL DESIGN

3.1 MACHINE DESCRIPTION

JT60-SA is an under-construction tokamak in Naka, Japan whose principal purpose is the contribution to early realization of fusion energy by supporting the exploitation and resolving key physics for ITER reactor.Figure 3.1 3.2

3.2 CREATE TOOLS

Consorzio di Ricerca per l' Energia, l' Automazione e le Tecnologie dell' Elettromagnetismo (CREATE)

3.3 CONTROLLER DESIGN

3.3.1 *eXtreme Shape Controller*

3.4 QST TOOLS IMPLEMENTATION

3.4.1 *CCS*

3.4.2 *QST magnetic controller (FBC)*

The QST magnetic controller FBC uses the PF coils signals to control the plasma current I_p and the FPPC coils signals for plasma position control.

QST magnetic controller calculates command values of active coil ccurrents/voltages from some information

$$I_{PF_ref}(t+\Delta t) = I_{PF}(t_0) + M_{PF}^{\dagger}\left[G_{SP}\delta\Psi_s(t) + G_{SI}\int_{t_0}^{t}\delta\Psi_s(t)dt + G_{XP}\delta\Psi_X(t) + G_{XI}\int_{t0}^{t}\delta\Psi_x(t)dt\right] \quad (3.1)$$

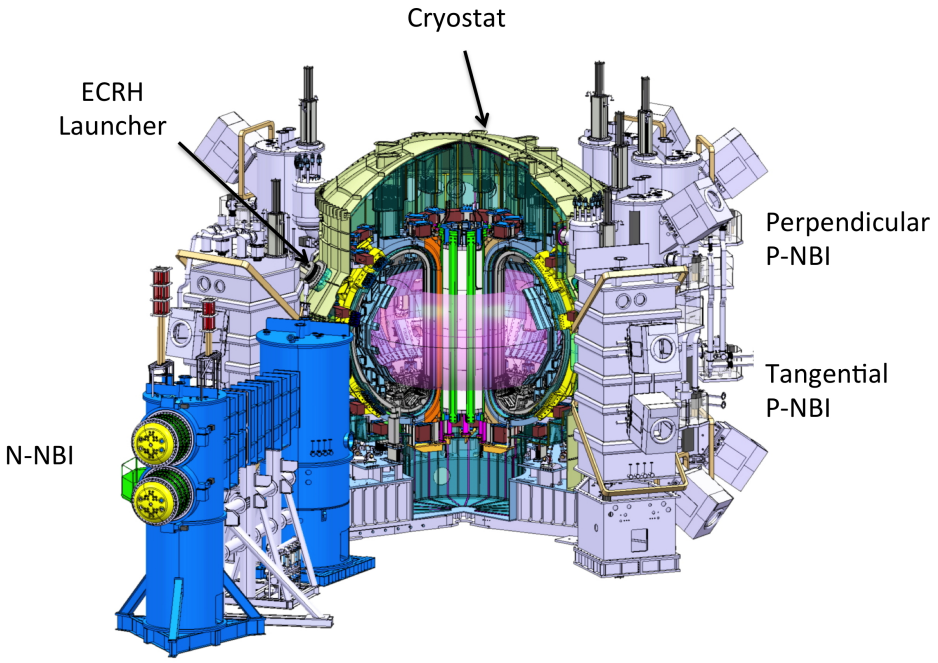

Figure 3.1.: JT60-SA tokamak configuration

$$V_{com} = G_{vt}\left[M_{coil}\frac{(I_{coil_ref} - I_{coil_meas})}{dt} + \frac{M_{plasma_now}\cdot I_{p_now} - M_{plasma_bfr}\cdot I_{p_bfr}}{dt}\right] \tag{3.2}$$

$$I_{FPPC_ref}(t+\Delta t) = I_{FPPC}(t_0) + M^{\dagger}_{FPPC}\left[G_{FP}\delta\Psi_{SF}(t) + G_{FD}\frac{d}{dt}\delta\Psi_{SF}(t)\right] \tag{3.3}$$

3.5 SIMULATION RESULTS

3.5.1 *ELM*

3.5.2 *Compound ELM*

3.5.3 *Minor Disruption*

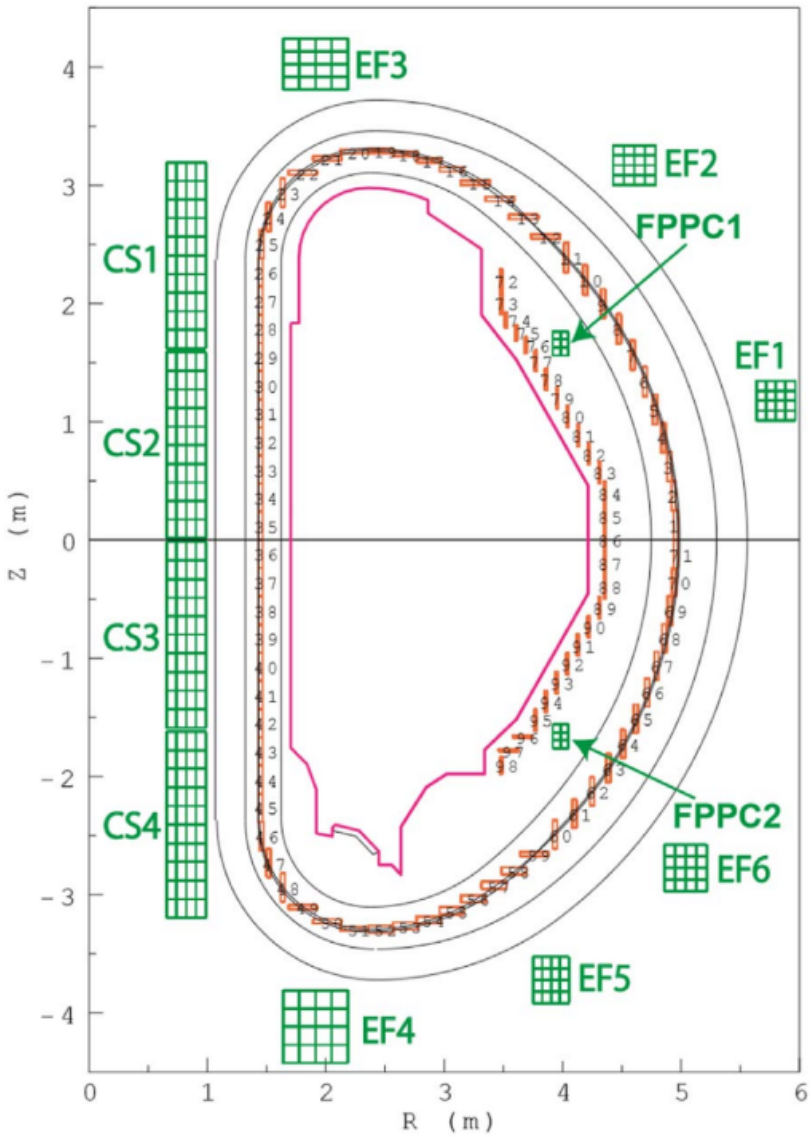

Figure 3.2.: JT-60SA poloidal cross-section and layout of the Poloidal Field coils system [14].

4

ISTTOK

4.1 MACHINE DESCRIPTION

4.2 DIAGNOSTICS AND ACTUATORS

4.3 ATCA-MIMO-ISOL BOARDS

4.3.1 *Hardware layout*

4.3.2 *Real-time integration software*

4.4 PLASMA CURRENT MAGNETIC FIELD

Retrieving the contribution of the plasma current in tokamaks ...

The methods of correction of the magnetic error fields due to inaccuracies of tokamak manufacturing and assembly are considered. The problems of the plasma position and shape reconstruction based on magnetic field measurements are discussed.

4.5 PLASMA CENTROID POSITION DETERMINATION

5

ISTTOK RESULTS

This chapter describes the latest implementations in ISTTOK MARTe framework followed by the presentation of the obtained results for control of the current centroid position.

5.1 IMPLEMENTATION OF THE GENERAL APPLICATION MODULES

General Application Modules (GAM)

5.1.1 *PID control implementation*

Proportional-Integrative-Derivative

5.1.2 *Data-driven state-space model retrieving*

Early efforts in finding a real-time equilibrium solver for ISTTOK were performed.

5.1.3 *Kalman filter implementation*

5.1.4 *Multiple-Input Multiple-Output control implementation*

5.2 PLASMA CURRUENT CENTROID POSITION CONTROL RESULTS

This section addresses the latest results from the real-time implementation of control algorithms in ISTTOK.

5.2.1 *PID control and LQR control results*

This section addresses obteined the experimental results in ISTTOK's plasma discharges.

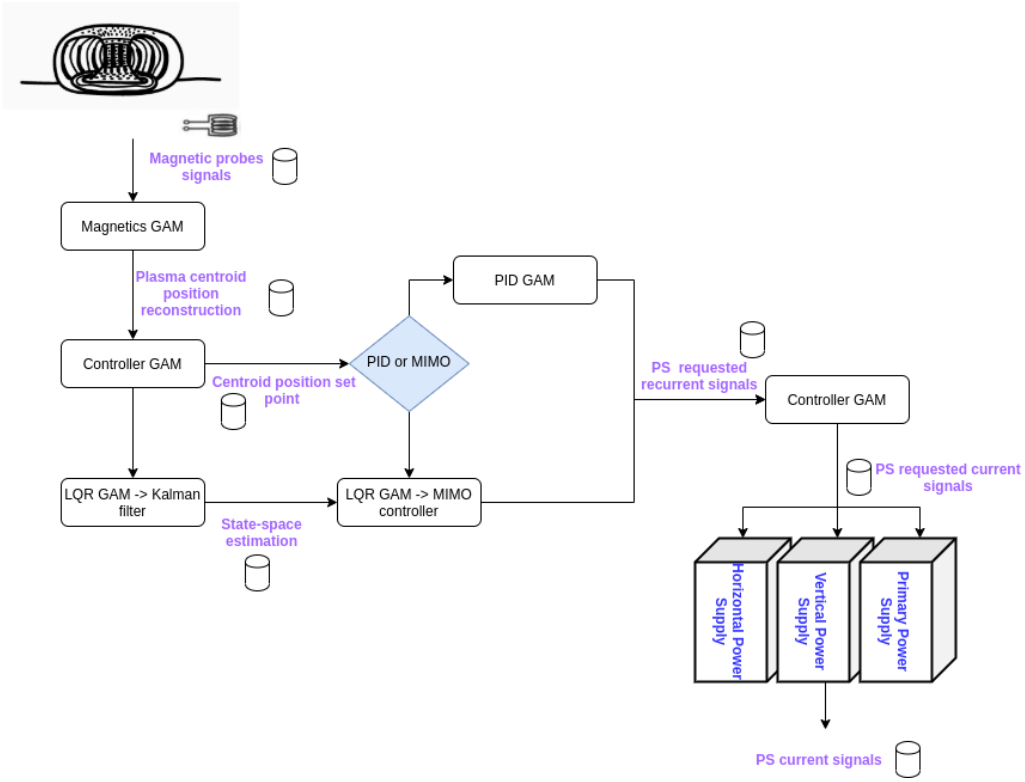

Figure 5.1.: ISTTOK MARTe overall scheme

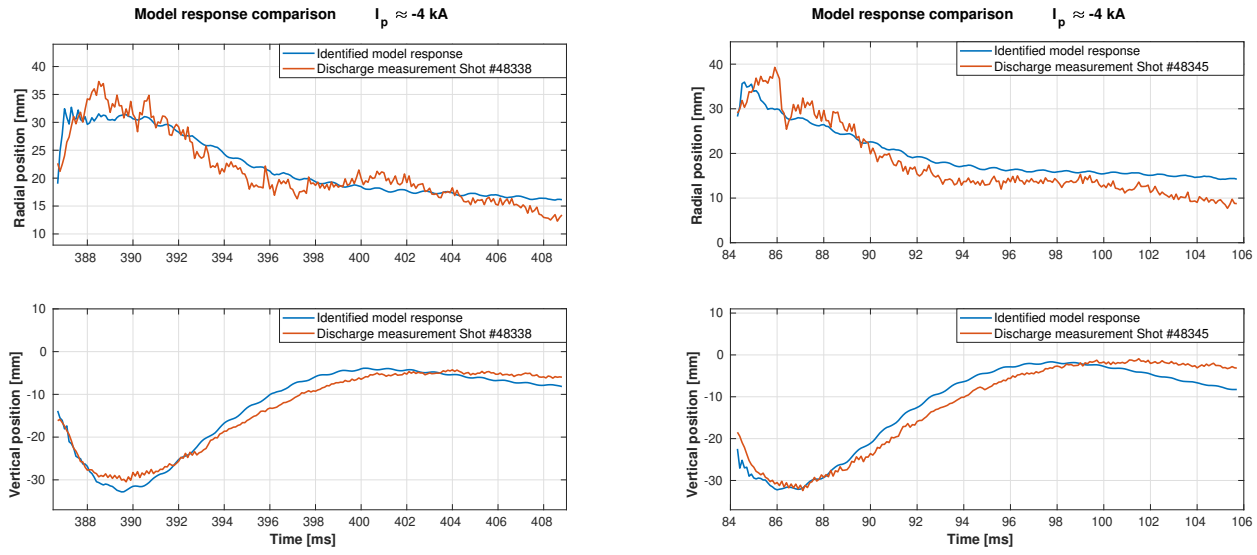

(a) (b)

Figure 5.2.: Fig.

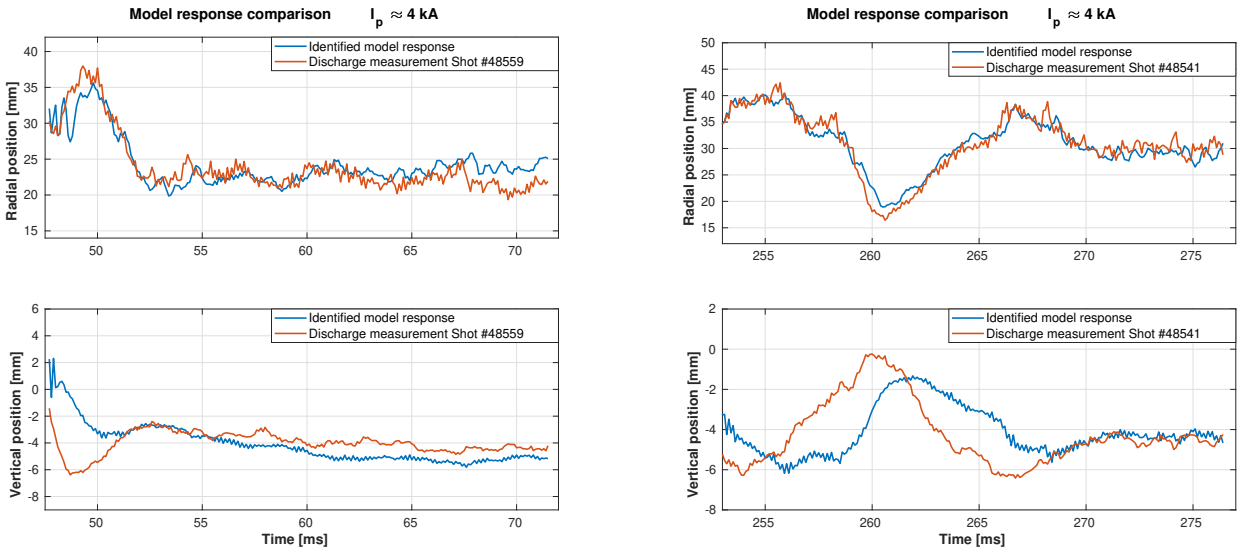

(a) (b)

Figure 5.3.: Fig.

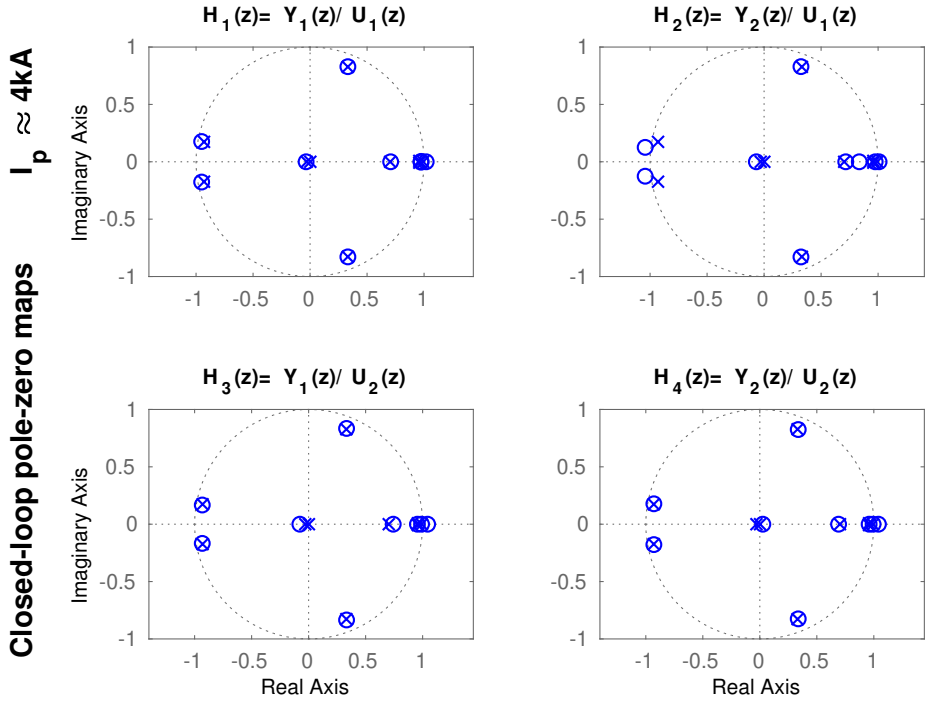

Figure 5.4.: Pole-Zero maps in closed loop for the model when $I_p \approx 4kA$. Superposition of poles and zeros can be seen in the four transfer functions.

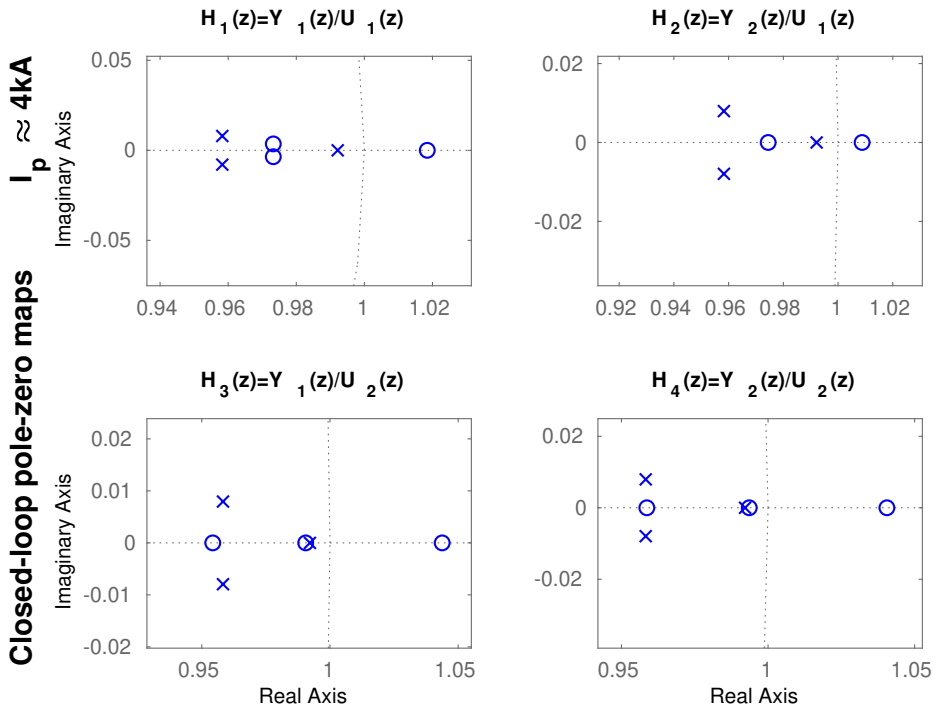
Closed-loop pole-zero maps
$I_p \approx 4kA$
$H_1(z)=Y_1(z)/U_1(z)$
$H_2(z)=Y_2(z)/U_1(z)$
$H_3(z)=Y_1(z)/U_2(z)$
$H_4(z)=Y_2(z)/U_2(z)$
Imaginary Axis
Real Axis

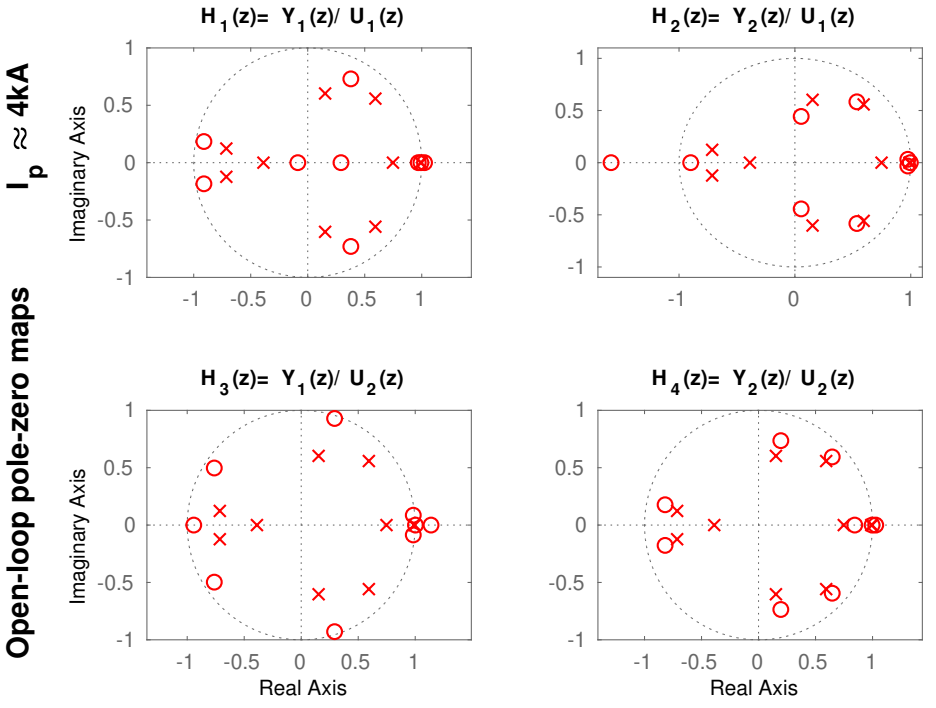
Open-loop pole-zero maps
$I_p \approx 4kA$
$H_1(z)= Y_1(z)/ U_1(z)$
$H_2(z)= Y_2(z)/ U_1(z)$
$H_3(z)= Y_1(z)/ U_2(z)$
$H_4(z)= Y_2(z)/ U_2(z)$
Imaginary Axis
Real Axis

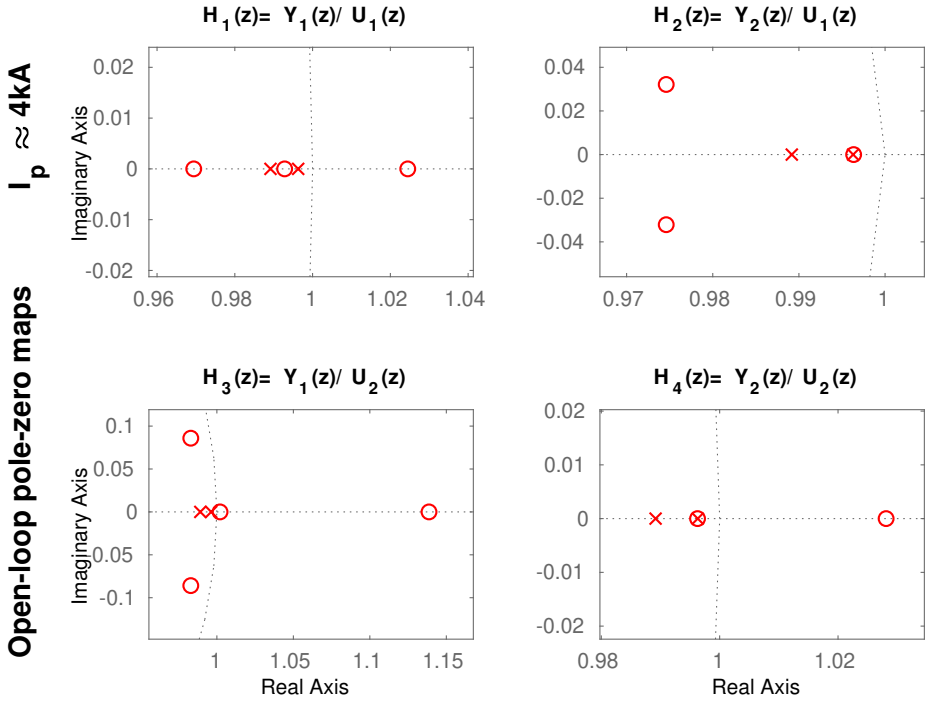
Open-loop pole-zero maps
$I_p \approx 4kA$
$H_1(z) = Y_1(z)/U_1(z)$
$H_2(z) = Y_2(z)/U_1(z)$
$H_3(z) = Y_1(z)/U_2(z)$
$H_4(z) = Y_2(z)/U_2(z)$
Imaginary Axis
Real Axis

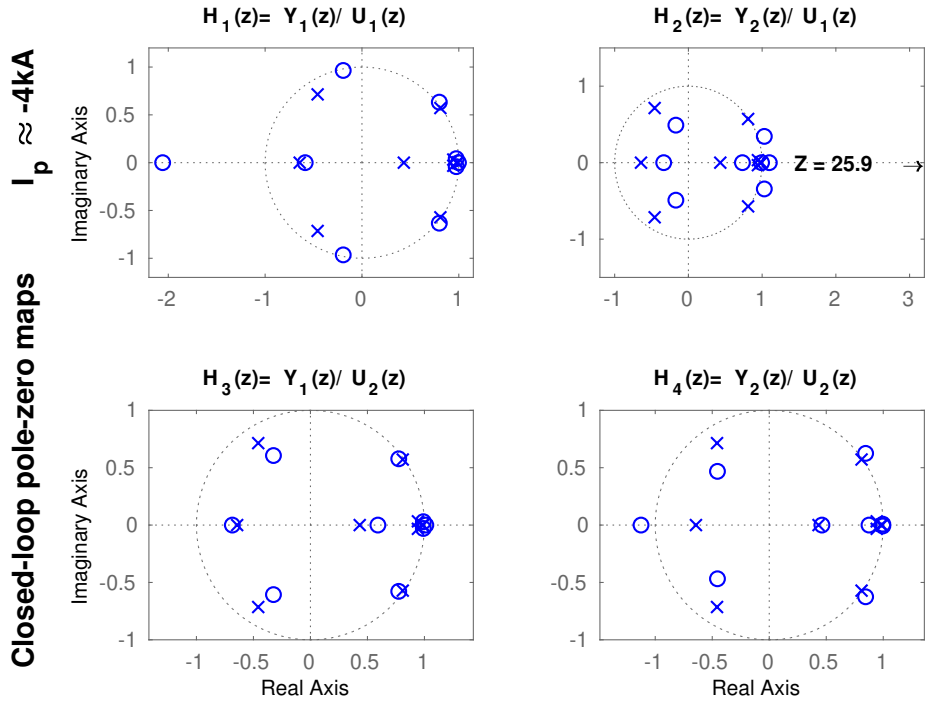
Closed-loop pole-zero maps
$I_p \approx -4kA$
$H_1(z) = Y_1(z)/U_1(z)$
$H_2(z) = Y_2(z)/U_1(z)$
Z = 25.9
$H_3(z) = Y_1(z)/U_2(z)$
$H_4(z) = Y_2(z)/U_2(z)$
Imaginary Axis
Real Axis

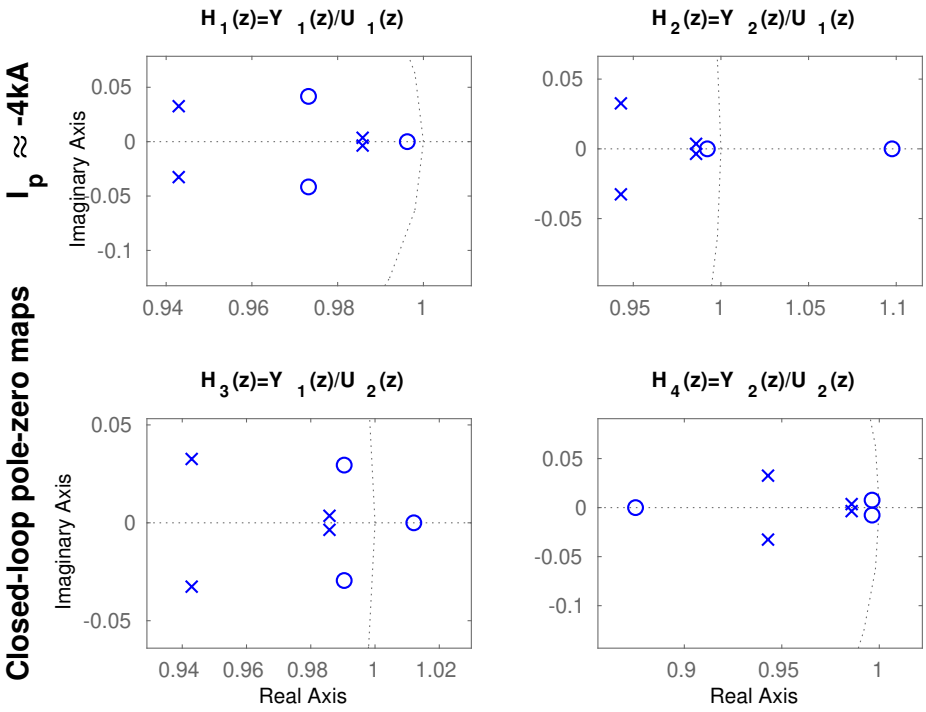
Closed-loop pole-zero maps
$I_p \approx -4kA$
$H_1(z)=Y_1(z)/U_1(z)$
$H_2(z)=Y_2(z)/U_1(z)$
$H_3(z)=Y_1(z)/U_2(z)$
$H_4(z)=Y_2(z)/U_2(z)$
Imaginary Axis
Real Axis

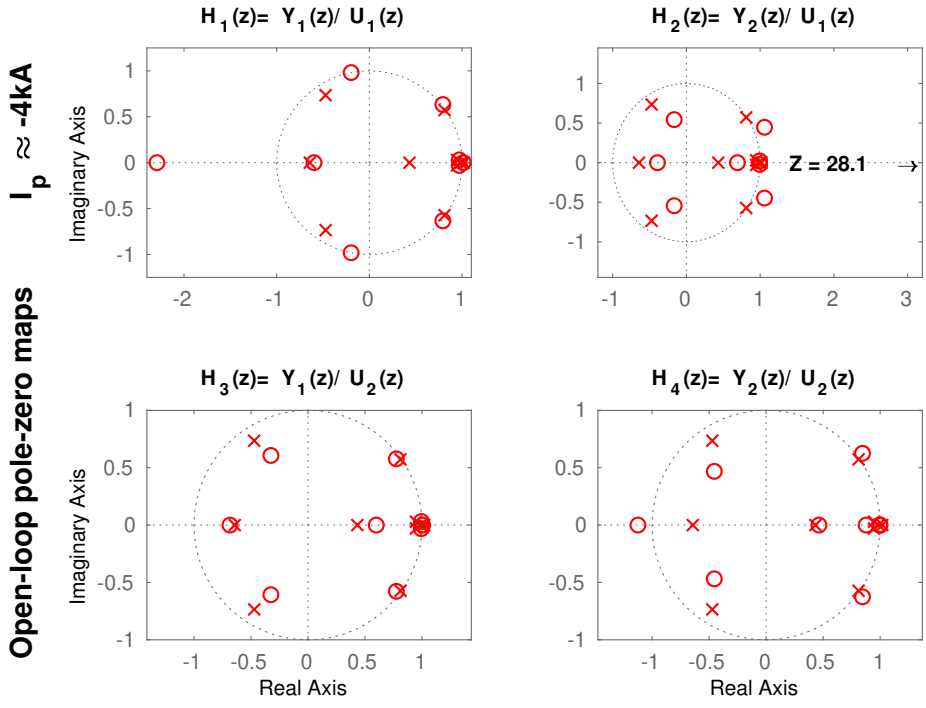
Open-loop pole-zero maps
$I_p \approx -4kA$
$H_1(z)= Y_1(z)/ U_1(z)$
$H_2(z)= Y_2(z)/ U_1(z)$
$H_3(z)= Y_1(z)/ U_2(z)$
$H_4(z)= Y_2(z)/ U_2(z)$
Z = 28.1
Imaginary Axis
Real Axis

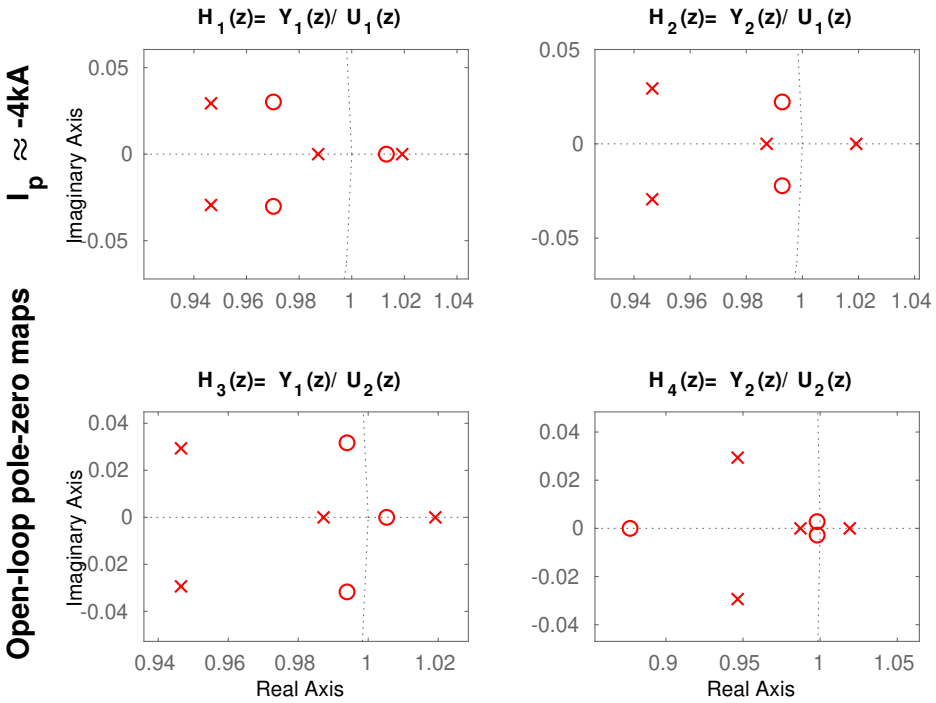
Open-loop pole-zero maps
$I_p \approx$ -4kA
$H_1(z) = Y_1(z)/U_1(z)$
$H_2(z) = Y_2(z)/U_1(z)$
$H_3(z) = Y_1(z)/U_2(z)$
$H_4(z) = Y_2(z)/U_2(z)$
Imaginary Axis
Real Axis

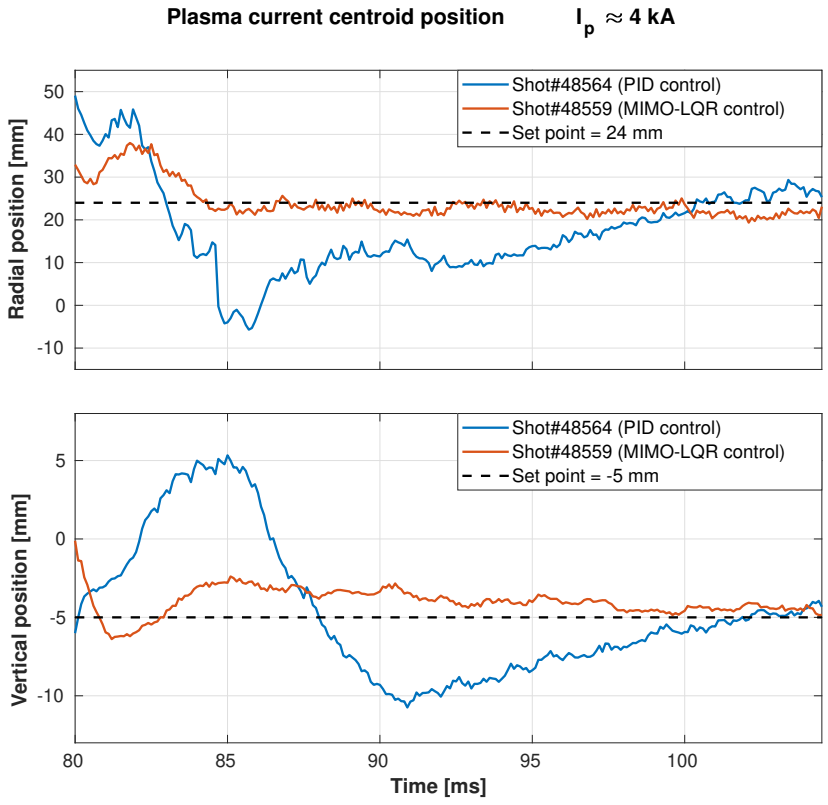
Plasma current centroid position
$I_p \approx$ 4 kA
Shot#48564 (PID control)
Shot#48559 (MIMO-LQR control)
Set point = 24 mm
Radial position [mm]
Set point = -5 mm
Vertical position [mm]
Time [ms]

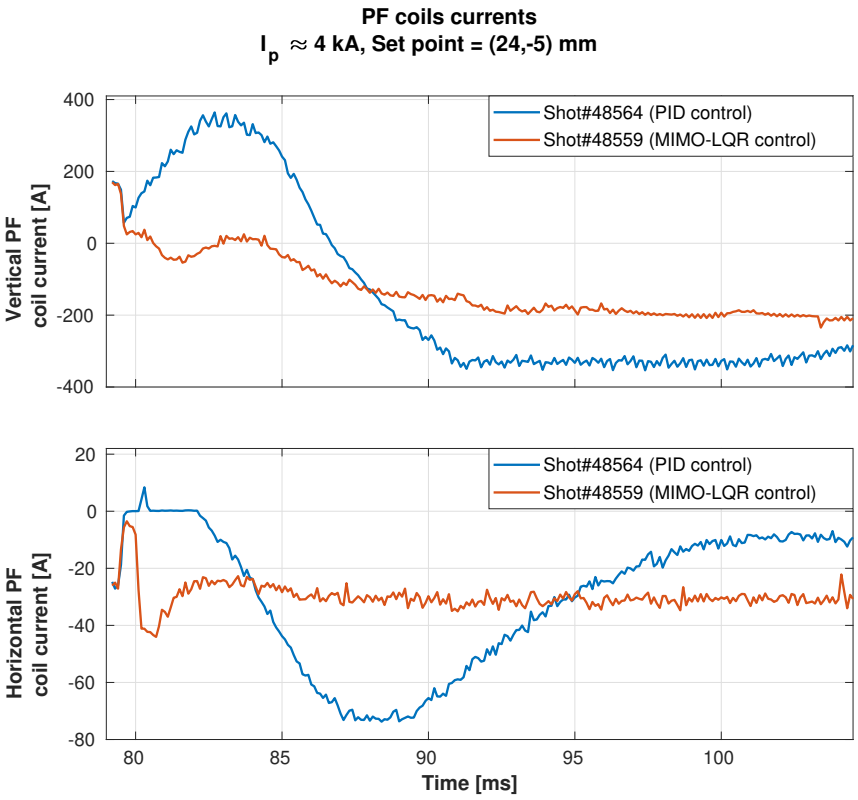
PF coils currents
$I_p \approx 4$ kA, Set point = (24,-5) mm
Shot#48564 (PID control)
Shot#48559 (MIMO-LQR control)
Vertical PF coil current [A]
Horizontal PF coil current [A]
Time [ms]

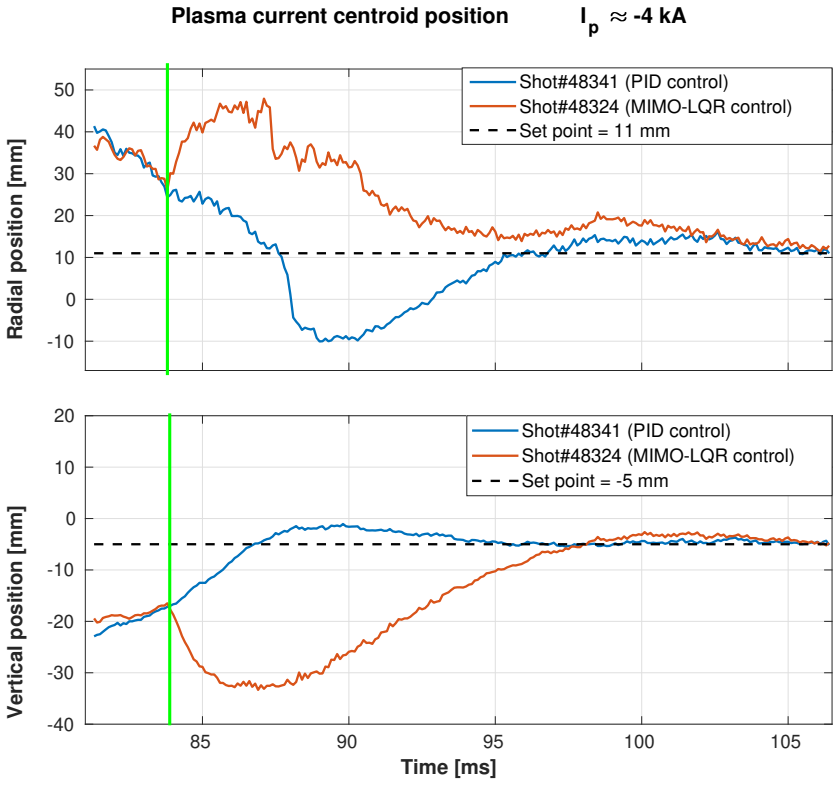
Plasma current centroid position
$I_p \approx -4$ kA
Shot#48341 (PID control)
Shot#48324 (MIMO-LQR control)
Set point = 11 mm
Set point = -5 mm
Radial position [mm]
Vertical position [mm]
Time [ms]

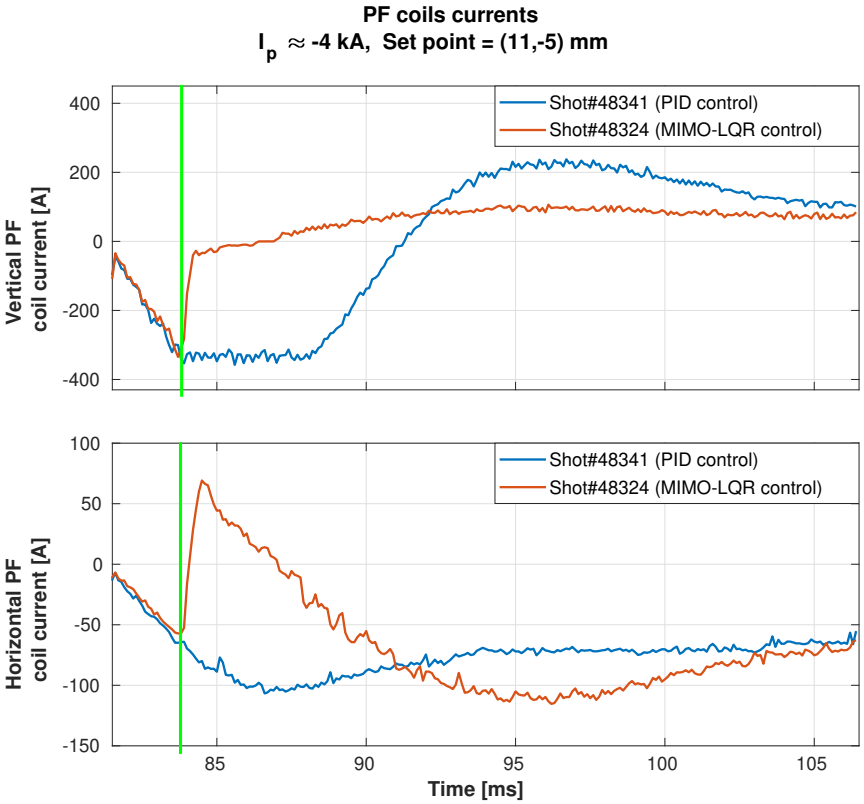

Control	Shot #	RMSE (R,z) mm	Set point (R,z) mm	I_p
PID	48564	(13.73, 4.4102)	(24, -5)	$\approx 4kA$
MIMO LQR	48559	(4.2252, 1.4215)	(24, -5)	$\approx 4kA$
PID	48563	(13.6717, 4.1652)	(24, -4)	$\approx 4kA$
MIMO LQR	48561	(8.1047, 3.2752)	(24, -4)	$\approx 4kA$
PID	48556	(12.0315, 3.3217)	(32, -5)	$\approx 4kA$
MIMO LQR	48555	(4.2618, 2.4698)	(32, -5)	$\approx 4kA$
PID	48551	(13.9998, 3.3431)	(27, -5)	$\approx 4kA$
MIMO LQR	48554	(5.9830, 2.0062)	(27, -5)	$\approx 4kA$
PID	48515	(6.0178, 2.6123)	(30, -5)	$\approx 4kA$
MIMO LQR	48541	(5.8372, 1.7664)	(30, -5)	$\approx 4kA$
PID	48544	(4.8745, 2.5167)	(32, -4)	$\approx 4kA$
MIMO LQR	48542	(4.4346, 3.6573)	(32, -4)	$\approx 4kA$
PID	48546	(11.4560, 3.4765)	(27, -7)	$\approx 4kA$
MIMO LQR	48548	(7.6745, 4.1569)	(27, -7)	$\approx 4kA$
PID	48341	(12.0959, 5.7652)	(11, -5)	$\approx -4kA$
MIMO LQR	48324	(15.4768, 14.3436)	(11, -5)	$\approx -4kA$

PID	48340	(11.7701, 5.9599)	(11.2, -5.5)	$\approx -4kA$
MIMO LQR	48338	(11.5260, 12.6226)	(11.2, -5.5)	$\approx -4kA$
PID	48343	(15.7675, 5.7453)	(12, -5)	$\approx -4kA$
MIMO LQR	48342	(14.5168, 14.4329)	(12, -5)	$\approx -4kA$
PID	48346	(12.4228, 6.1541)	(12.2, -5.3)	$\approx -4kA$
MIMO LQR	48345	(9.7513, 13.0338)	(12.2, -5.3)	$\approx -4kA$
PID	48349	(19.3397, 5.5406)	(11.5, -5.6)	$\approx -4kA$
MIMO LQR	48348	(9.1727, 13.1505)	(11.5, -5.6)	$\approx -4kA$
PID	48352	(15.2181, 6.5395)	(10.8, -4.7)	$\approx -4kA$
MIMO LQR	48354	(14.6405, 13.7307)	(10.8, -4.7)	$\approx -4kA$
PID	48351	(13.4078, 5.8769)	(13.2, -5.6)	$\approx -4kA$
MIMO LQR	48350	(13.9320, 14.4940)	(13.2, -5.6)	$\approx -4kA$

Table 5.1.: Centroid position RMSE comparison between PID and MIMO-LQR controlled discharges for different set points and plasma current scenarios.

6

CONCLUSIONS

bla bla bla

BIBLIOGRAPHY

[1] Andrej A. Kavin Valerij A. Belyakov. *Fundamentals of Magnetic Thermonuclear Reactor Design*. Elsevier, 2018.

[2] J. R. Ferron, A. Kellman, E. McKee, T. Osborne, P. Petrach, T. S. Taylor, J. Wight, and E. Lazarus. An advanced plasma control system for the diii-d tokamak. In *[Proceedings] The 14th IEEE/NPSS Symposium Fusion Engineering*, pages 761–764 vol.2, Sep. 1991.

[3] B. G. Penaflor, J. R. Ferron, A. W. Hyatt, M. L. Walker, R. D. Johnson, D. A. Piglowski, E. Kolemen, A. S. Welander, and M. J. Lanctot. Latest advancements in DIII-D Plasma Control software and hardware. *2013 IEEE 25th Symposium on Fusion Engineering, SOFE 2013*, pages 1–4, 2013.

[4] M. Margo, B. Penaflor, H. Shen, J. Ferron, D. Piglowski, P. Nguyen, J. Rauch, M. Clement, A. Battey, and C. Rea. Current State of DIII-D Plasma Control System. *Fusion Engineering and Design*, 150(October 2019), 2020.

[5] Mellanox Technologies. Introduction to InfiniBand. Technical report, 2003.

[6] J. I. Paley, S. Coda, B. Duval, F. Felici, and J. M. Moret. Architecture and commissioning of the TCV distributed feedback control system. *Conference Record - 2010 17th IEEE-NPSS Real Time Conference, RT10*, pages 1–6, 2010.

[7] H. Anand, C. Galperti, S. Coda, B. P. Duval, F. Felici, T. Blanken, E. Maljaars, J. M. Moret, O. Sauter, T. P. Goodman, and D. Kim. Distributed digital real-time control system for the TCV tokamak and its applications. *Nuclear Fusion*, 57(5), 2017.

[8] A. C. Neto, F. Sartori, F. Piccolo, R. Vitelli, G. De Tommasi, L. Zabeo, A. Barbalace, H. Fernandes, D. F. Valcarcel, and A. J. N. Batista. Marte: A multiplatform real-time framework. *IEEE Transactions on Nuclear Science*, 57(2):479–486, April 2010.

[9] G. De Tommasi, F. Piccolo, A. Pironti, and F. Sartori. A flexible software for real-time control in nuclear fusion experiments. *Control Engineering Practice*, 14(11):1387–1393, 2006.

[10] André C. Neto, Diogo Alves, Luca Boncagni, Pedro J. Carvalho, Daniel F. Valcárcel, Antonio Barbalace, Gianmaria De Tommasi, Horácio Fernandes, Filippo Sartori, Enzo Vitale, Riccardo Vitelli, and Luca Zabeo. A survey of recent MARTe based systems. In *IEEE Transactions on Nuclear Science*, volume 58, pages 1482–1489, 2011.

[11] A Neto, D Alves, B B Carvalho, P J Carvalho, H Fernandes, D F Valc, G De Tommasi, Associazione Euratom-enea create, Via Claudio, P Mccullen, A Stephen, Euratom-ccfe Fusion Association, Culham Science Centre, Abingdon Ox, United Kingdom, R Vitelli, Tor Vergata, Via Politecnico, L Zabeo, and Iter Organisation. Marte Framework : a Middleware for Real-Time Applications Development. In *13th International Conference on Accelerator and Large Experimental Physics Control Systems*, number 11, pages 1277–1280, Grenoble, France, 2011.

[12] Andre C. Neto, Filippo Sartori, Riccardo Vitelli, Llorenc Capella, Giuseppe Ferro, Ivan Herrero, and Hector Novella. An agile quality assurance framework for the development of fusion real-Time applications. In *2016 IEEE-NPSS Real Time Conference, RT 2016*, 2016.

[13] Chiara Piron, Gabriele Manduchi, Paolo Bettini, Federico Felici, Claudio Finotti, Paolo Franz, Ondrej Kudlacek, Giuseppe Marchiori, Lionello Marrelli, J. M. Moret, Paolo Piovesan, Olivier Sauter, and Cesare Taliercio. Integration of the state observer RAPTOR in the real-time MARTe framework at RFX-mod. *Fusion Engineering and Design*, 123:616–619, 2017.

[14] N Cruz, G. De Tommasi, M Mattei, A Mele, Y Miyata, A Pironti, and T Suzuki. Control-oriented tools for the design and validation of the JT-60SA magnetic control system. *Control Engineering Practice*, 63:81–90, 2017.

A

EXTENDED CONTROL RESULTS

This appendix contains the corresponding plots of the ISTTOK discharges from table 5.2.1.

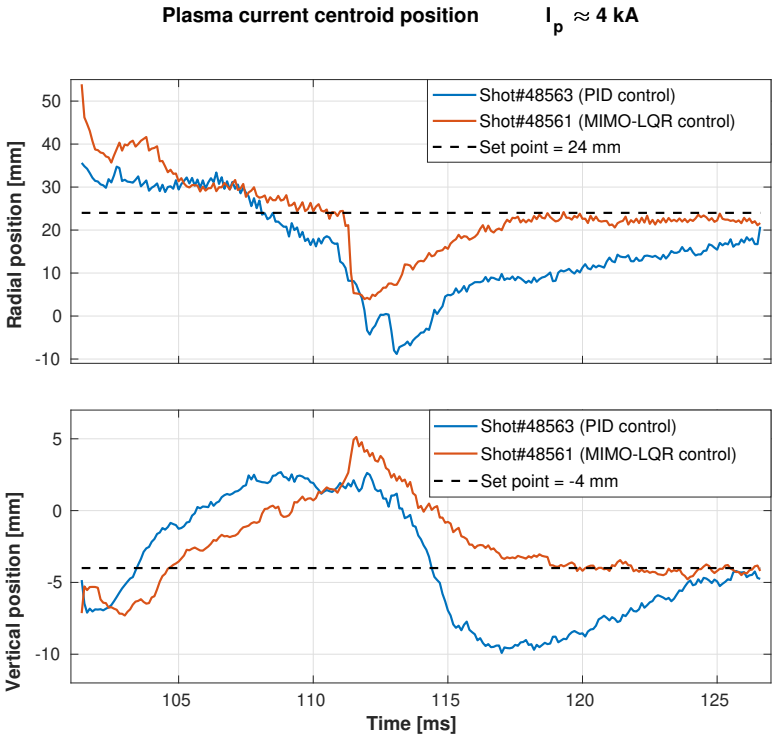

Figure A.1.: Plasma centroid position Shot# 48563 Shot# 48561

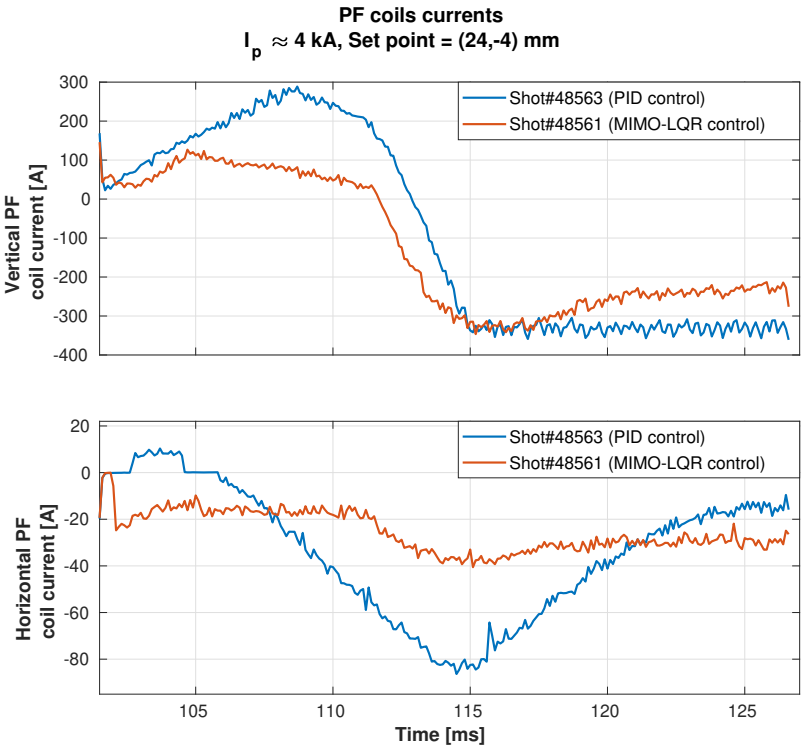

Figure A.2.: lalala Shot# 48563 Shot# 48561

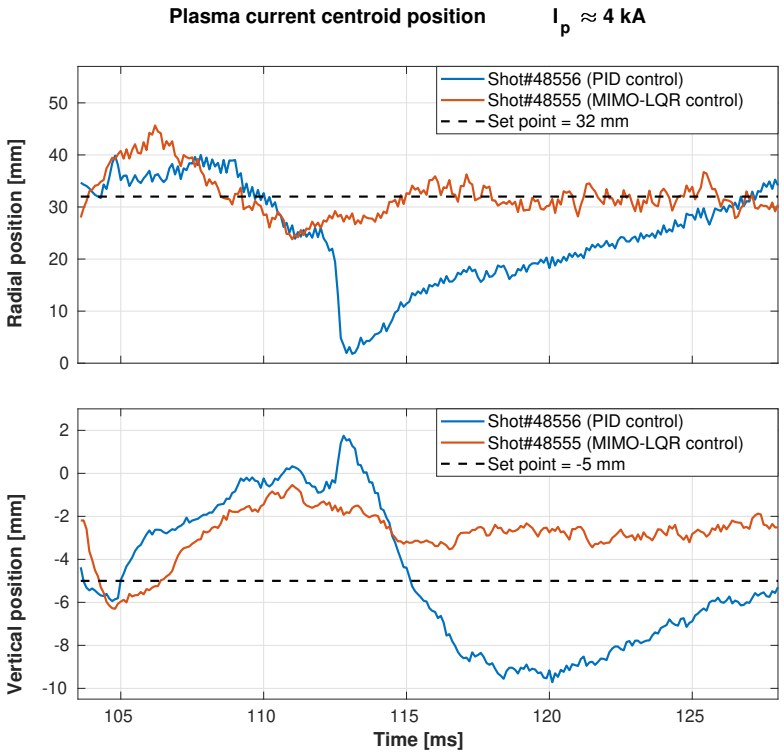

Figure A.3.: Plasma centroid position Shot# 48556 Shot# 48552

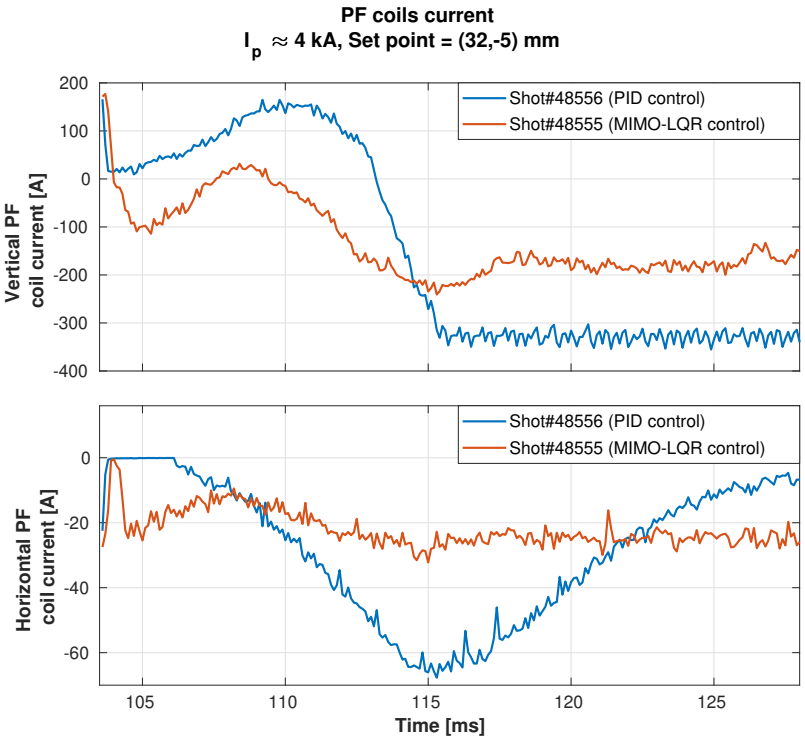

Figure A.4.: lalala Shot# 48556 Shot# 48552

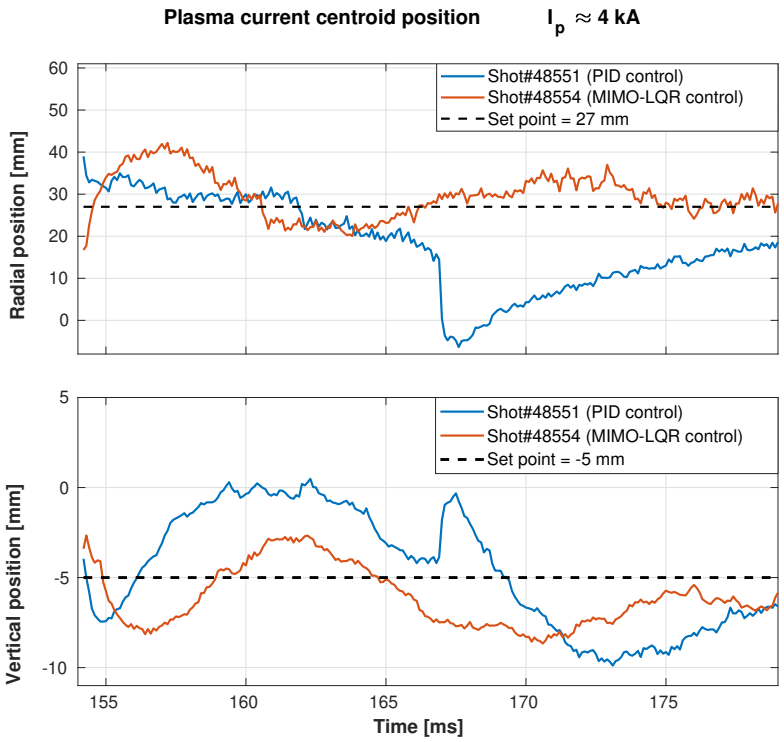

Figure A.5.: Plasma centroid position Shot# 48551 Shot# 48554

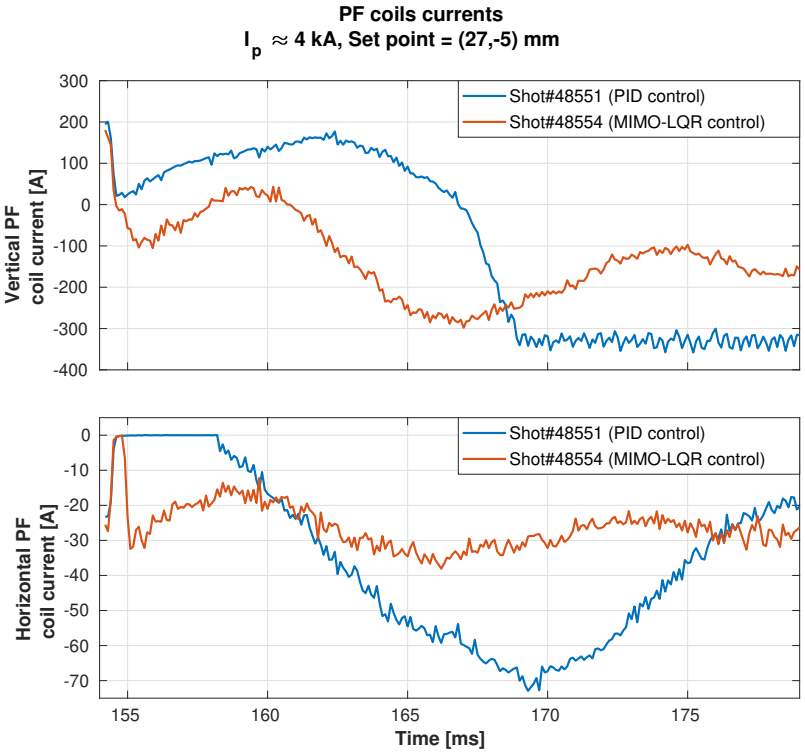

Figure A.6.: lalala Shot# 48551 Shot# 48554

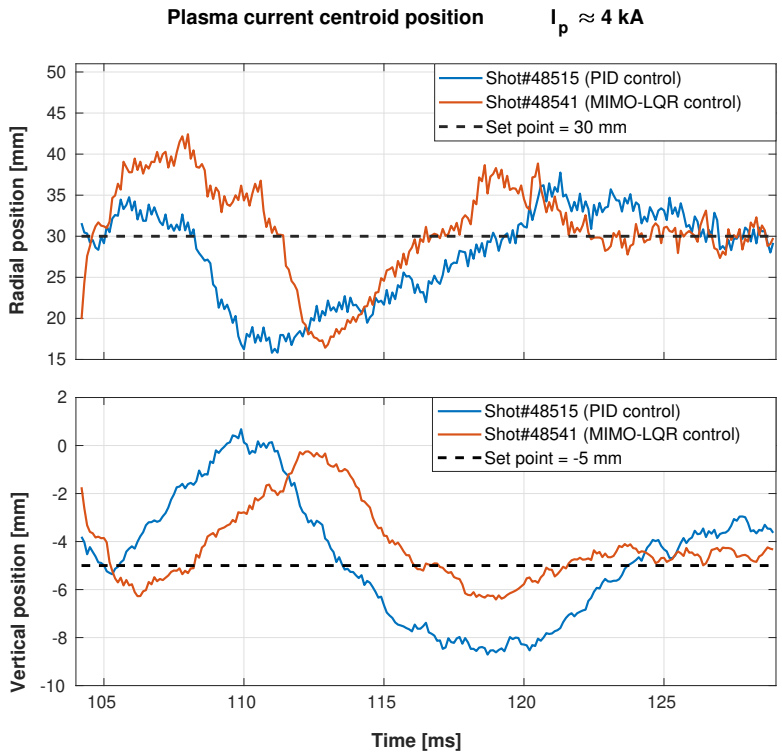

Figure A.7.: Plasma centroid position Shot# 48515 Shot# 48541

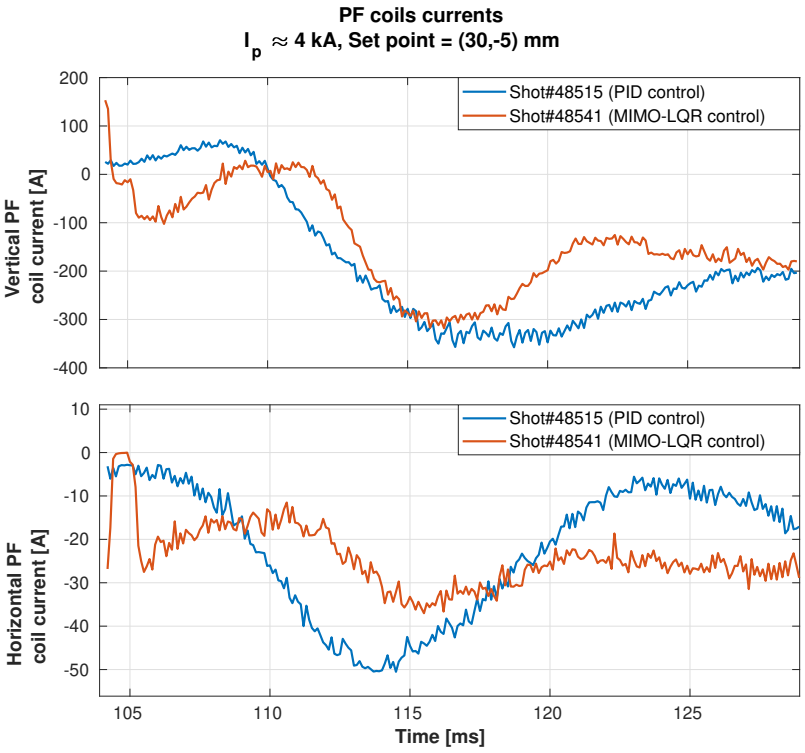

Figure A.8.: lalala Shot# 48515 Shot# 48541

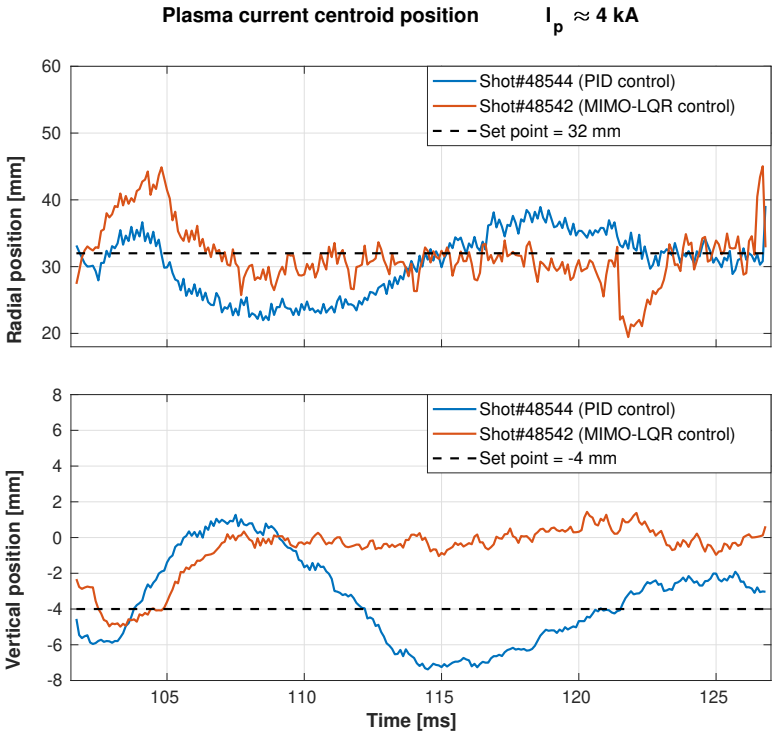

Figure A.9.: Plasma centroid position Shot# 48544 Shot# 48542

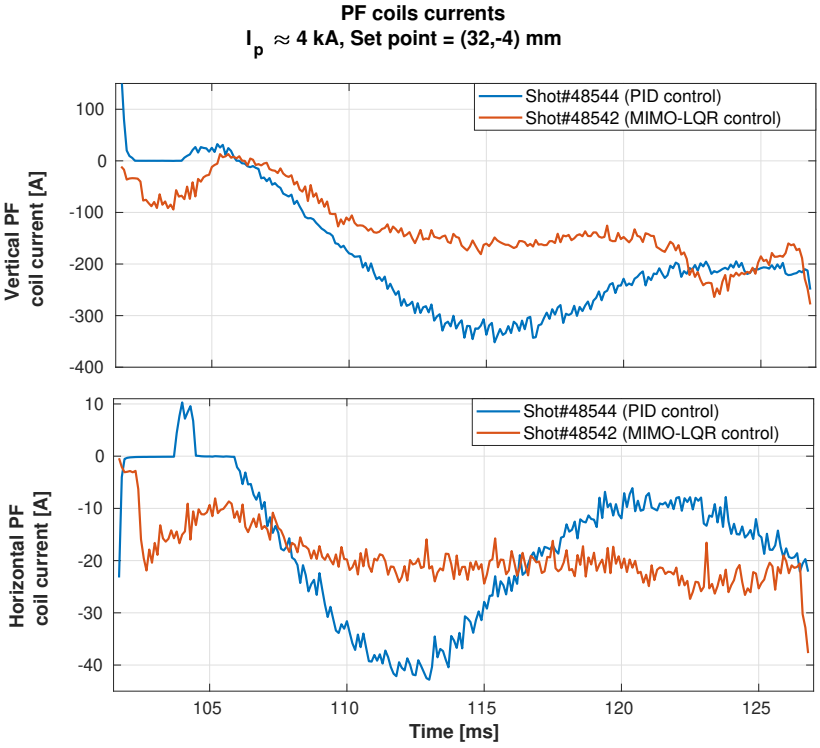

Figure A.10.: lalala Shot# 48544 Shot# 48542

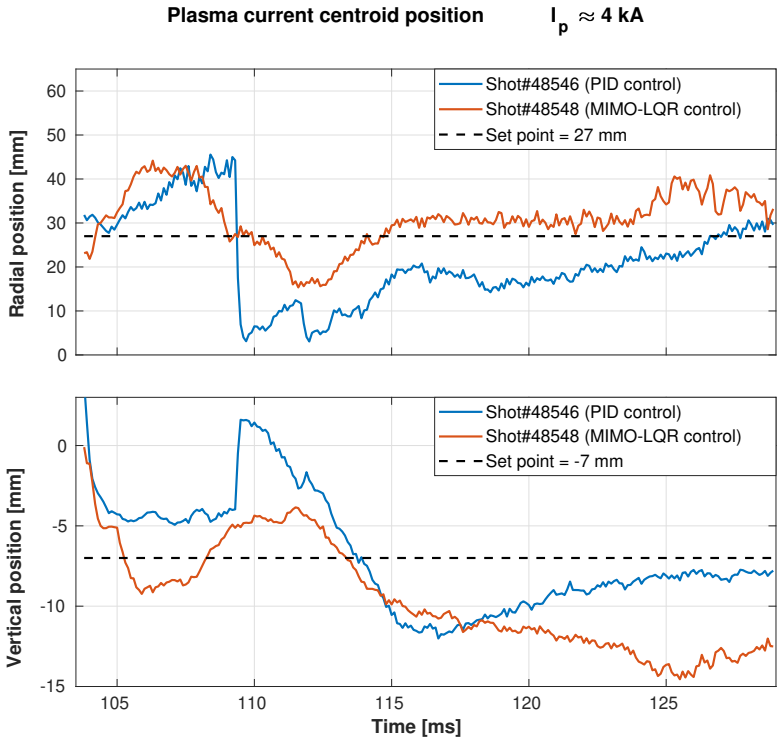

Figure A.11.: Plasma centroid position Shot# 48546 Shot# 48548

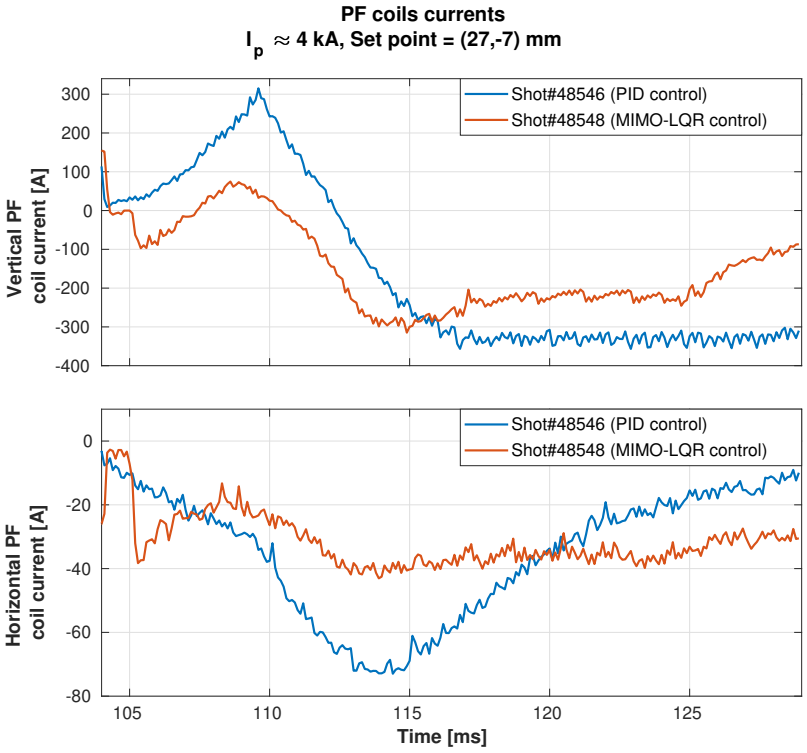

Figure A.12.: lalala Shot# 48546 Shot# 48548

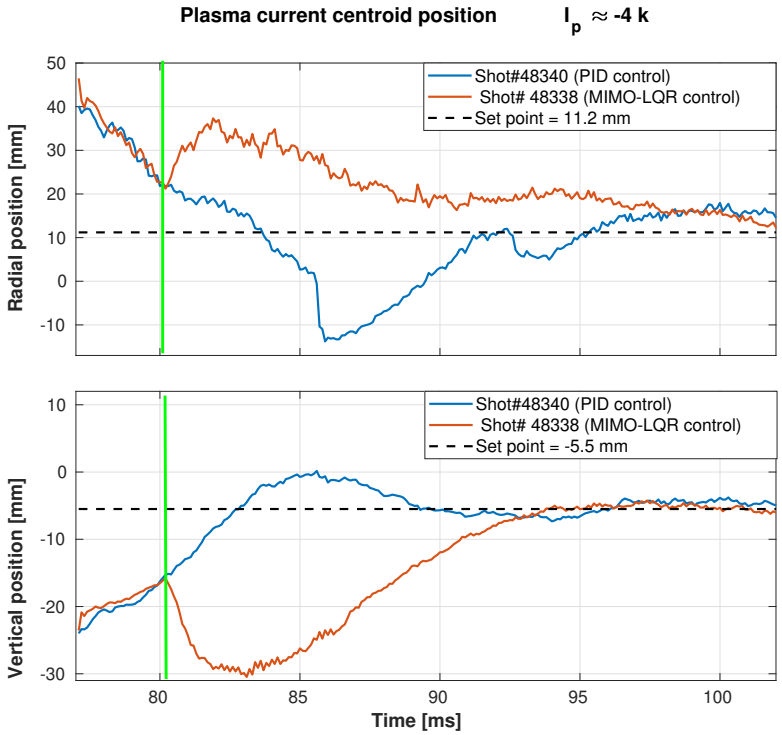

Figure A.13.: Plasma centroid position Shot# 48340 Shot# 48338

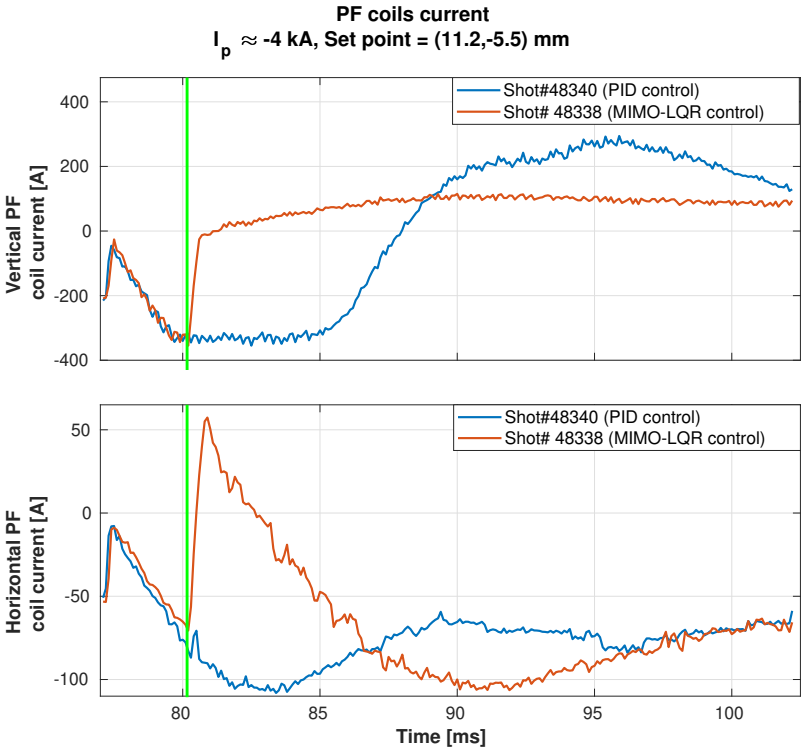

Figure A.14.: lalala Shot# 48340 Shot# 48338

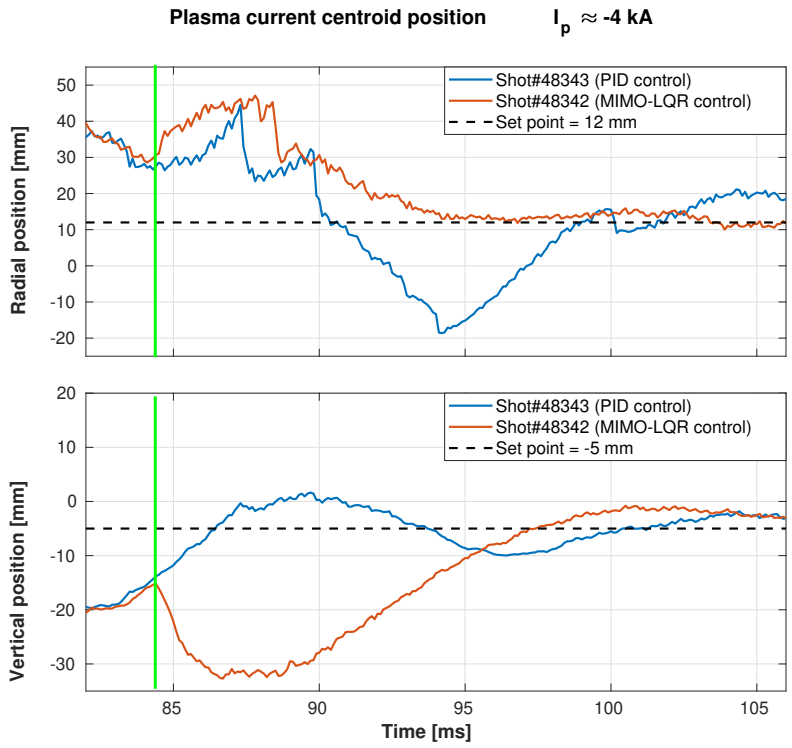

Figure A.15.: Plasma centroid position Shot# 48343 Shot# 48342

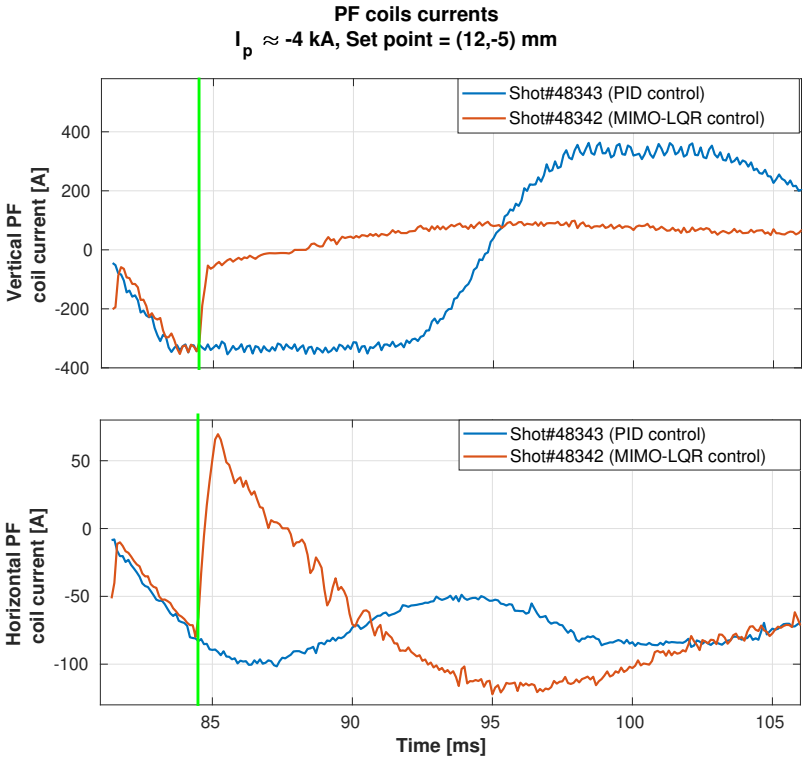

Figure A.16.: lalala Shot# 48343 Shot# 48342

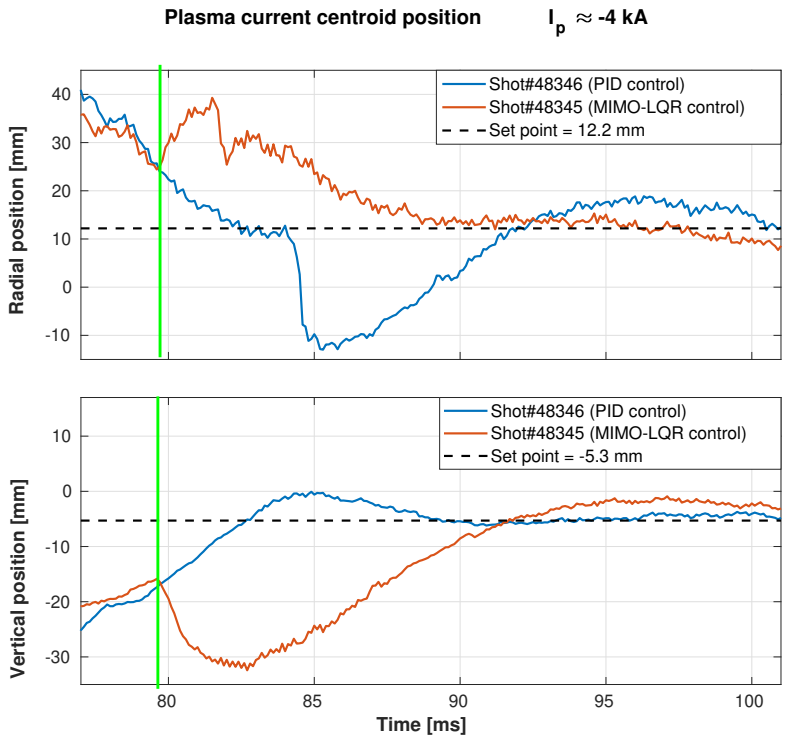

Figure A.17.: Plasma centroid position Shot# 48346 Shot# 48345

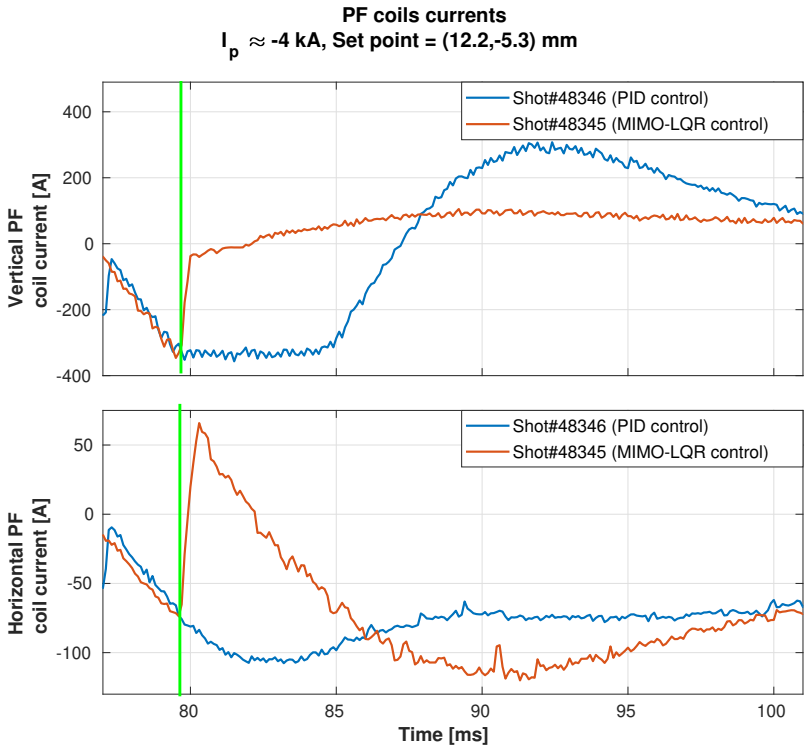

Figure A.18.: lalala Shot# 48346 Shot# 48345

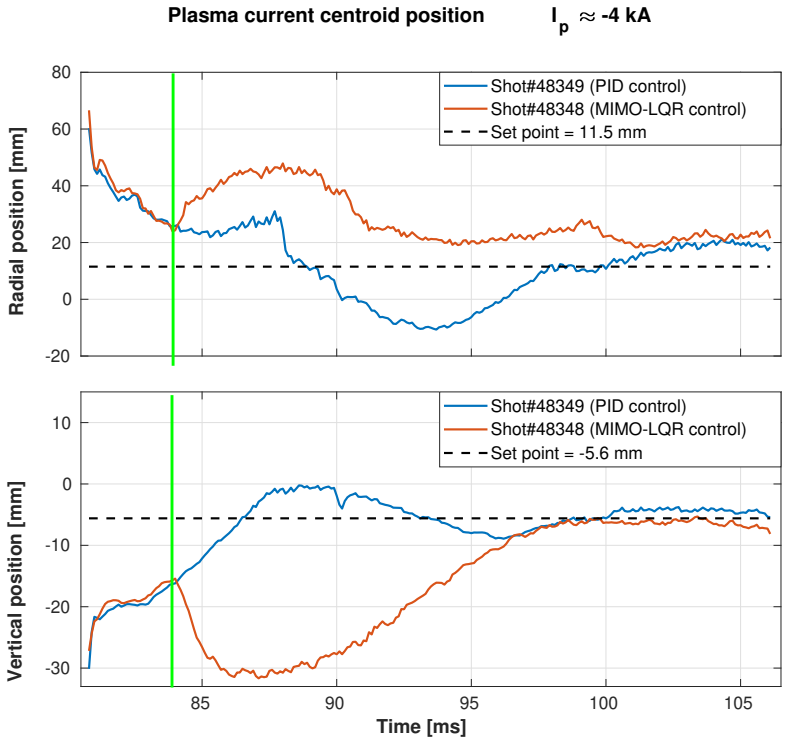

Figure A.19.: Plasma centroid position Shot# 48349 Shot# 48348

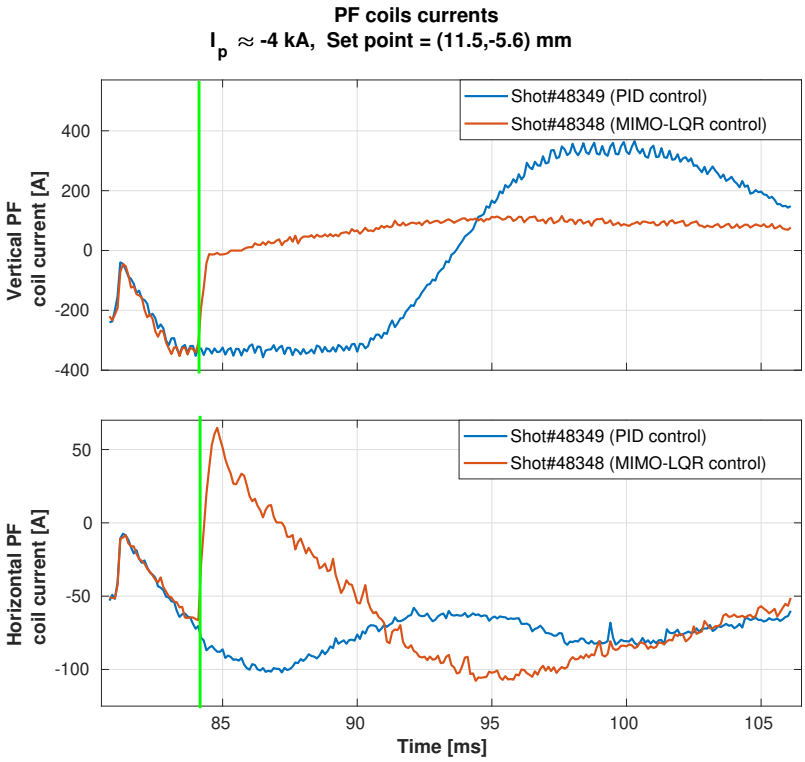

Figure A.20.: lalala Shot# 48349 Shot# 48348

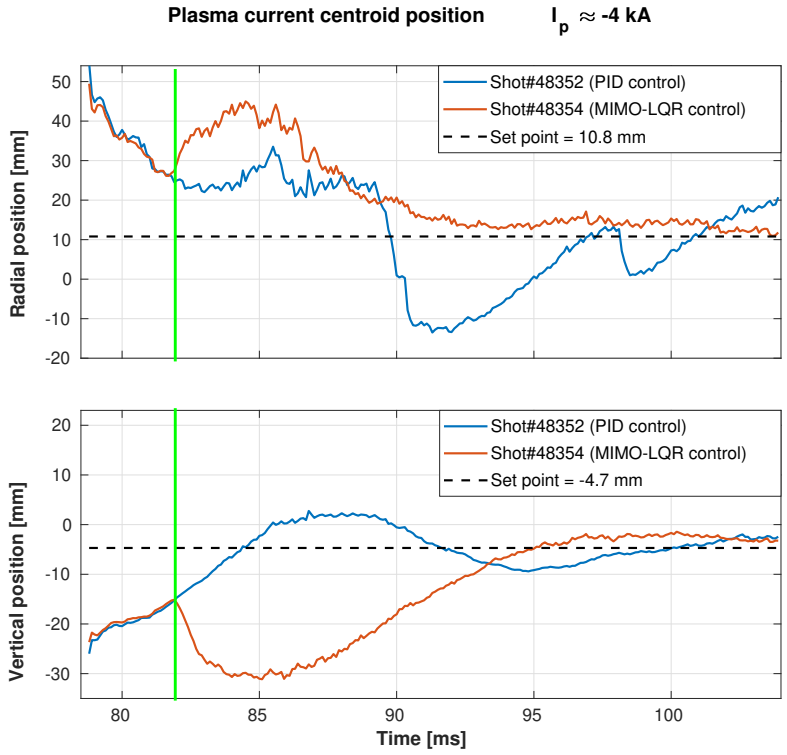

Figure A.21.: Plasma centroid position Shot# 48352 Shot# 48354

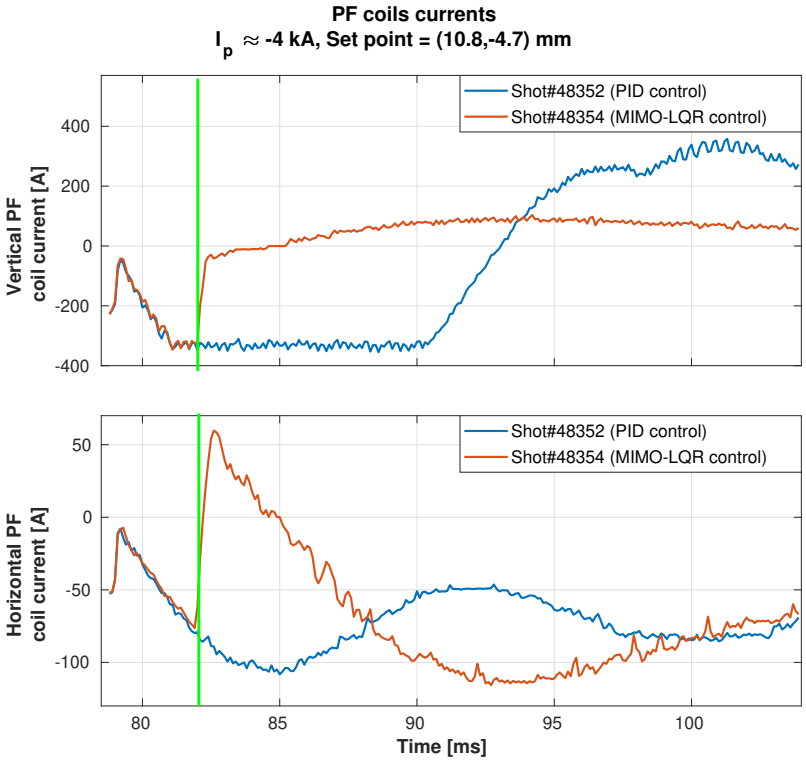

Figure A.22.: lalala Shot# 48352 Shot# 48354

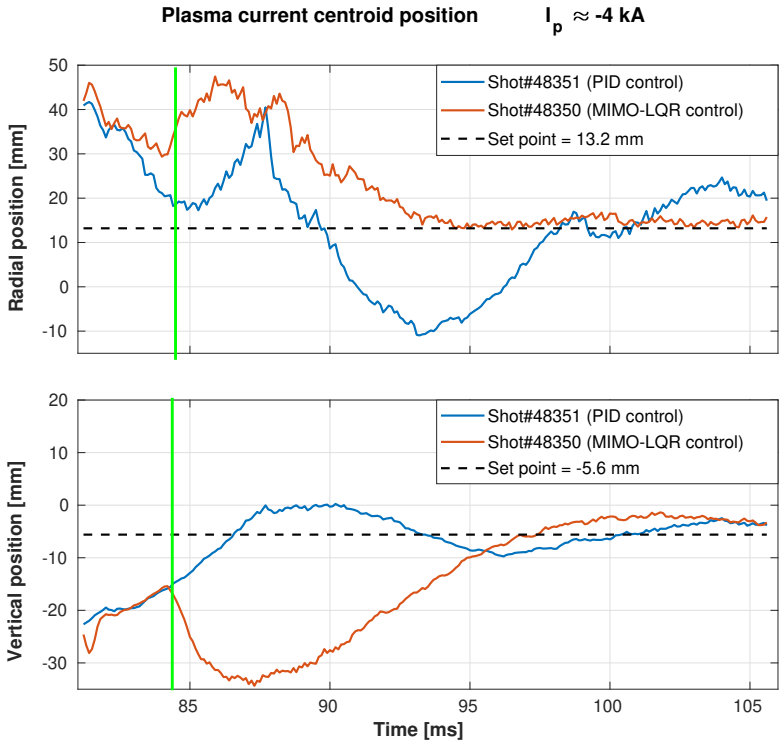

Figure A.23.: Plasma centroid position Shot# 48351 Shot# 48350

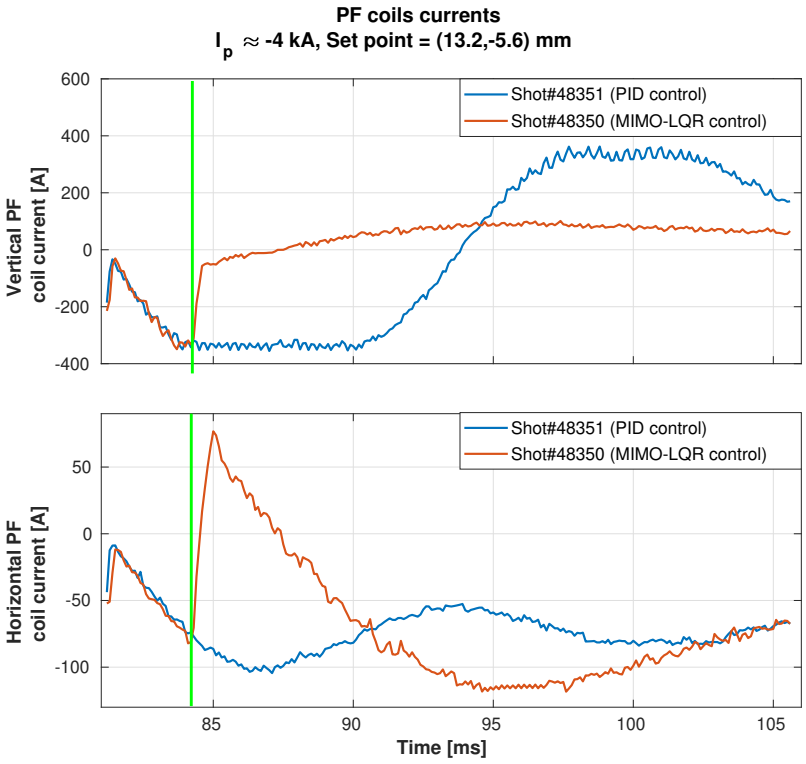

Figure A.24.: lalala Shot# 48351 Shot# 48350

B

FBC CONTROLLER AND CCS CONFIGURATION